A Comparative Analysis of Solar Parabolic Dish Driven Recompression S-CO_2 Brayton Cycles with and without Reheat

Muhammad Sajid Khan

Submitted to the
Institute of Graduate Studies and Research
in partial fulfillment of the requirements for the degree of

Master of Science
in
Mechanical Engineering

Eastern Mediterranean University
January 2018
Gazimağusa, North Cyprus

Approval of the Institute of Graduate Studies and Research

Assoc. Prof. Dr. Ali Hakan Ulusoy
Acting Director

I certify that this thesis satisfies the requirements as a thesis for the degree of Master of Science in Mechanical Engineering.

Prof. Dr. Hasan Hacisevki
Chair, Department of Mechanical Engineering

We certify that we have read this thesis and that in our opinion it is fully adequate, in scope and quality, as a thesis of the degree of Master of Science in Mechanical Engineering.

Prof. Dr. Uğur Atikol
Supervisor

Examining Committee

1. Prof. Dr. Uğur Atikol

2. Prof. Dr. Fuat Egelioglu

3. Asst. Prof. Dr. Roozbeh Vaziri

ABSTRACT

The current study presents a thermodynamic comparison between two different supercritical carbon dioxide (S-CO_2) Brayton cycles integrated with parabolic dish solar system. Recompression S-CO_2 Brayton cycles with reheat and without reheat are examined for their net power output, cycle efficiencies as well as integrated system efficiencies. The analyses are conducted by developing a comprehensive mathematical code in Engineering Equation Solver (EES). Parabolic dish system is assessed and optimized on the basis of yearly available data and by using the optimization results, a thorough comparative study based on thermal efficiencies, integrated system efficiencies and work output is carried out. The system comprises of indirect heated Brayton cycle in which fresh water is utilized as a heat transfer fluid in solar collector, whereas, Brayton cycle comprised of S-CO_2. The dish system is designed by taking the average annual direct normal irradiance (DNI) 1000 W/m^2 approximately and such system is effective for southern part of Pakistan, Cyprus and Spain and many other countries where sun shines almost nine to eleven hours daily and DNI varies from 700 to 1000 W/m^2.

The outcomes of the research state that the recompression with reheat S-CO_2 Brayton cycle has achieved thermal efficiency almost 47.70%, while the other system has nearly 45.02%. The recompression with reheat cycle has an overall energy efficiency of almost 30.37 % however the recompression without reheat system has almost 27.5%. Furthermore, second law integrated efficiency of recompression without reheat system is almost 29.6%, whereas, reheating system has 32.7% overall exergetic efficiency. Reheating has improved efficiency almost 10.5 %. The effect of increase

in minimum cycle temperature is positive for reheat system and the efficiency tends to be reduced due to the increase in main compressor work for without reheat system. Moreover, the effect of rise in pressure ratio on integrated system performance is similar to that of minimum cycle temperature influence. Exergy destruction rate of collector receiver is approximately 40% which reduces with increase in the inlet temperature of the compressor, whereas, recuperators and pre cooler has more exergy losses than other components.

Keywords: Parabolic dish system, S-CO_2, Brayton cycle, Energy and Exergy efficiency, Pressure ratio, Net power output, minimum cycle temperature.

ÖZ

Mevcut çalışma, parabolik çanak güneş sistemi ile entegre edilmiş iki farklı süper kritik karbon dioksit (S-CO_2) Brayton döngüsü arasındaki termodinamik bir karşılaştırmayı sunmaktadır. Tekrar ısıtmalı ve yeniden ısıtmalı rekompresyon S-CO_2 Brayton devreleri, net güç çıkışı, çevrim verimliliği ve entegre sistem verimleri açısından incelendi. Analizler, Mühendislik Denklem Çözücü (EES) 'de kapsamlı bir matematiksel kod geliştirerek gerçekleştirildi. Parabolik çanak sistemi, yıllık verilere dayanarak değerlendirdi ve optimize edildi ve optimizasyon sonuçlarını kullanarak, termal verimlilik, entegre sistem verimliliği ve iş çıkışı üzerine kapsamlı bir karşılaştırmalı çalışma yürütüldü. Sistem, güneş kolektöründe taze suyun bir ısı transfer sıvısı olarak kullanıldığı dolaylı ısıtmalı Brayton çevriminden oluşurken Brayton çevrimi S-CO_2'den oluşur. Çanak sistemi, yılda yaklaşık ortalama 1000 W / m2'lik yıllık ortalama doğrudan ışınım alarak dizayn edilmiş ve bu sistem, Güney Pakistan, Kıbrıs ve İspanya'nın ve güneşin neredeyse dokuz saat ila on saat aralıklarla parladığı diğer birçok ülkede etkili.

Araştırma sonuçlarına göre, S-CO_2 Brayton tekrar ısıtma sistemi ile yapılan rekompresyon, yaklaşık% 47.70 oranında termik verimlilik elde ederken diğer sistem yaklaşık% 45.02'ye ulaştı. Yeniden ısıtma çevrimi ile yapılan rekompresyon genel enerji verimliliğine yaklaşık % 30.37 sahiptir, ancak yeniden ısıtma sistemi olmayan rekompresyon yaklaşık % 27.5'tir. Dahası, yeniden ısıtma sistemi olmayan rekompresyonun ikinci yasaya entegre etkinliği yaklaşık% 29.6, buna karşılık yeniden ısıtma sistemi% 32.7'lik ekserjetik etkinliğe sahiptir. Yeniden ısıtma verimliliği neredeyse% 10.5 arttı. Yeniden ısıtma sistemi için minimum çevrim sıcaklığındaki

artışın etkisi olumlu olmakla birlikte, yeniden ısıtma sistemi olmadan, ana kompresör çalışmasındaki artışa bağlı olarak verimlilik azalma eğilimi gösterir. Dahası, basınç oranındaki artışın tümleşik sistem performansına etkisi, minimum çevrim sıcaklığının etkisine benzer. Kollektör alıcısının Exergy imha oranı yaklaşık% 40'dır ve kompresör giriş sıcaklığındaki artışla birlikte azalırken, reküpatörler ve ön soğutucu da büyük ekserji kayıplarına sahiptir.

Anahtar Kelimeler: Parabolik çanak sistemi, S-CO_2, Brayton çevrimi, Enerji ve ekserji verimi, Basınç oranı, Net güç çıkışı, minimum çevrim sıcaklığı.

DEDICATION

Dedicated to

my wife who has always been supportive of me during my time at EMU

and

my parents.

ACKNOWLEDGMENT

I thank to Allah Almighty for the blessings and awarding me the patience to complete my work successfully. I hope that Allah will always help me in the future.

My special thanks go to my supervisor Prof. Dr. Ugur Atikol for his invaluable feedback, guidance, encouragement and understanding at the most difficult times. I am also grateful to the members of the thesis jury, Prof. Dr. Fuat Egelioglu and Asst. Prof. Dr. Roozbeh Vaziri for their helpful suggestions and comments. Their reviews, comments and feedback made me feel that I am accomplishing a meaningful task.

I would also like to thank Asst. Prof. Dr. Nilgun Hancioglu for her help and guidance during the course of "Thesis Writing for the Post Graduate Students", and rectifying the grammatical mistakes, which enabled me to complete my thesis.

Last but not least, a heartfelt thanks to my wife and parents, for their trust, encouragement and support at every stage.

TABLE OF CONTENTS

LIST OF TABLES

LIST OF FIGURES

LIST OF SYMBOLS AND ABBREVIATIONS

A	Area (m^2)
A_a	Aperture area (m^2)
A_r	Receiver area (m^2)
C	Concentration Ratio
C_p	Specific Heat Capacity (J/kg-K)
d	Diameter of the Receiver (m)
DNI	Direct Normal Irradiation (W/m^2)
E	East
e_x	Specific Exergy (kJ/kg)
F_R	Heat Removal Factor
G_b	Solar Intensity Radiation (W/m^2)
h	Specific Enthalpy (kJ/kg)
HTR	High Temperature Recuperator
LTR	Low Temperature Recuperator
$\dot{m}$	Mass Flow Rate through S-CO_2 Cycle (kg/sec)
N	North
PDSC	Parabolic Dish Solar Collector
$\dot{Q}_u$	Thermal Energy (kW)
R	Radius of the Aperture (m)
S	Absorbed Solar Radiation (W/m^2)
S-CO_2	Super Critical Carbon Dioxide
SCRBC	Supercritical Carbon Dioxide Recompression Brayton Cycle
T	Temperature (K)

TIT	Turbine Inlet Temperature (K)
U	Overall Heat Loss ($W/m^2.K$)
$\dot{W}$	Work Output (kW)
$\dot{X}$	Rate of Exergy (kW)
x	Recompressed Mass Fraction
$\dot{\psi}$	Exergy Destruction Rate (kW)
ε	Effectiveness of Heat Exchangers
η	Efficiency

Subscripts

a	Aperture
dest	Destruction
en	Energy
HPT	High Pressure Turbine
l	Loss
LPT	Low Pressure Turbine
Mc	Main Compressor
ov	Overall
pc	Pre-Cooler
pet	Patella
Recomp	Recompressor
r	Receiver
S	Source
sun	Sun
tot	Total
tur	Turbine

th	Thermal
U	useful
0	Dead State (Environmental)
1, 2, 3---	State Points

Chapter 1

INTRODUCTION

1.1 Background

Energy is considered as a basic source in the generation of prosperity and plays a considerable role in social and economic development of any society. The requirement for energy is increasing rapidly while the conventional energy resources (oil, coal etc.) are being depleted gradually. These conventional energy resources create environmental problems as well as the destruction of infrastructures. Recently, three main ecological problems (acid rain, ozone layer depletion and global warming), which are caused by the burning of conventional energy resources, and are threatening to the environment. Therefore, to eliminate these harmful elements from our environment, use of fossil fuels needs to be replaced by renewable energy resources as much as possible.

Renewable energy resources such as solar, geothermal, wind and biomass can be good alternatives to the traditional energy resources. In addition, renewable energy resources are environmentally friendly, pollution free, available in abundant quantities almost throughout the whole world. Among the renewable resources, solar energy has the greatest advantage as clean and pollution free energy which can be converted directly or indirectly for power generation requirements. Recently two main solar technologies are being used for power generation, photovoltaic and solar thermal power. In photovoltaic system sun energy is directly converted into electricity with the

use of photovoltaic materials. However the updated technology uses heat exchangers and turbines (steam or gas) to generate electricity from solar radiations. Different types of sustainable power production systems were assessed on cost basis and discussed by [1, 2].

The reduction in the cost of electricity generated by the nuclear power plants is an important step that describes the better use of nuclear power. To achieve this purpose, all efforts have concentrated towards the simplicity and lower cost of primary power generation systems. Therefore a power cycle that can achieve high efficiency with less fuel consumption has been desired. Furthermore, a closed gas turbine cycles have simplicity, compactness and low cost with shorter construction duration in comparison with the steam cycles.

Helium Brayton cycle as the most sophisticated cycle among the closed gas turbine cycles has suggested by Dostal [3]. However, it has a drawback, in which it needs core outlet temperature of almost 900 $^{\circ}$C (1173 K) to gain the thermal efficiency (45-48 %). The high temperature surroundings that has needed for helium cycles and for other gas cycles is a challenge to its constructional material as they can be deformed at such higher temperatures. Thus, a power conversion cycle that would be able to get greater thermal efficiency at temperatures between 500 °C and 700 °C (773 K - 973 K) has been desired by the researchers. The main drawback of an ideal cycle such as helium cycle in compare with the supercritical CO_2 is the increment in compression work.

Therefore Feher [4] suggested that supercritical CO_2 closed loop cycles are the most favorable power generation systems which can reach high efficiency. S-CO_2 has compared to the critical points of different fluids given in Table 1. Due to the inertness,

balanced critical pressure value, stabilization, non-flammability, low cost and for its thermodynamics properties, CO_2 is selected among the wide range of working fluids.

Table 1.1: Critical Values of Various Fluids.

Fluid Name	Formula	Critical Temperature (°C)	Critical Pressure (M Pa)
Ammonia	NH_3	132.89	11.28
Carbon Dioxide	CO_2	30.98	7.38
Sulfur Dioxide	SO_2	157.50	7.88
Sulfur Hexafluoride	SF_6	45.56	3.76
Water	H_2O	373.89	22.10
Xenon	Xe	16.61	5.88

If a cycle is rejecting heat at lower temperature then it has capability to get higher thermal efficiency from thermodynamic point of view [5]. Thus, the critical temperature should be in a range so that the working fluid can work properly. Furthermore, another reason of using CO_2 in non-condensing cycles is the maximum temperature difference availability which could enable this cycle to get the highest efficiency.

Concentrated solar power technologies consist of various types of solar to thermal conversion techniques including parabolic trough (PT) system, parabolic dish (PD) system, linear Fresnal and solar power tower (helio state) [6]. All these systems convert the energy of solar radiations into thermal heat which can be further utilizes for power production [7] by integrating them to different steam and gas cycles.

In contrast with the other concentrated solar power (CSP) technologies (Parabolic trough, Linear Fresnal and Power tower), Parabolic dish has not been considered for power generation applications by the Scholars. For a dish system integrated with S-CO_2 Brayton cycles, the performance of the integrated system under different operating conditions should be investigated.

1.2 Thesis Objectives

The aim of current research is to investigate and compare the performance of the recompression S-CO_2 Brayton cycles with and without reheat and their integration with parabolic dish solar system.

1.3 Significance of the Study

The proposed solar thermal power system can be used for electricity generation in areas where, solar irradiations are quite high and other sources of power generation are not feasible.

1.4 Thesis Overview

Chapter 2 reviews the literature on the concentrated solar power technologies and their integration with power cycles and identifies the research gap in this field. Chapter 3 shows details about parabolic dish system and its integration with two different S-CO_2 Brayton cycles with the help of schematic and T-s diagrams. Chapter 4 presents the complete mathematical modeling and simulation of the systems that has employed in this research with the help of Engineering Equation Solver (EES). Chapter 5 illustrates the outcomes of the research in detail and the validation of the current study with the published data. Finally, Chapter 6 is based on the conclusions of the whole dissertation and it also consists of the suggestions for future work.

Chapter 2

LITERATURE REVIEW

Parabolic dish collectors are one of the emerging technologies solar thermal power plants that are used for power production. This system has an advantage as compared to the conventional collector systems as cosine losses do not consider here that was stated by Palavras and Bakos [8]. Since the beginning of 1970s dish-based solar thermal power plants have been used by the Australian National University (ANU). A 20 m^2 dish was constructed and tested by supplying power to a remote village as discussed in [9]. In 1994 a prototype of 400 m^2 dish that is known as a Big Dish having 50 kWe steam engine was completed by ANU. For solar thermal power generation applications, Abid et al. [10] showed that parabolic dish system has an advantage over parabolic trough system. The overall exergy as well as outlet temperature of parabolic dish (PD) collectors are higher as compared to parabolic trough (PT) solar collectors.

Supercritical CO_2 Brayton cycles are prominent effective technologies having cycle thermal efficiencies of almost 50%. When these gas cycles are integrated with solar systems, they can exhibit better performance and higher thermal efficiencies due to the greater concentration ratio which was depicted by Ho and Iverson [11]. Furthermore, CO_2 was suggested as a working fluid with supercritical cycles integrated with solar power thermal systems by Song et al. [12] as well as Organic Rankine Cycle in waste heat applications [13]. The supercritical CO_2 Brayton cycle is considered as a power cycle for solar system applications. Turchi et al. [14] stated that the initial cost of S-

CO_2 Brayton cycle is lower than other power cycles and can get better performance at higher temperatures. The supercritical carbon dioxide is a better conversion option for the nuclear reactors [15] due to its simplicity, safety and better economy as compared with the steam and helium based power cycles.

Feher [16] suggested CO_2 as a working fluid in a supercritical power cycle that achieved efficiency of almost 55% under ideal situations. Energy and exergy analysis of S-CO_2 recompression Brayton cycle was performed by Sarkar [17]. He concluded that heat exchangers have more irreversibilities than turbo machineries. The optimization of pressure ratio and intermediate pressure between both turbines for S-CO_2 recompression with reheat cycle was performed by Sarkar and Bhattacharyya [18]. Exergeoeconomic analysis of a combined cycle was assessed by Akbari and Mahmoudi [19], by using several organic fluids in which topping cycle consists of S-CO_2 cycle, whereas, organic Rankine cycle is bottoming cycle. They concluded that the second law efficiency of super critical recompression Brayton cycle (SCRBC) is lower than that of combined cycle. Niu et al. [20] studied experimentally under different flow conditions of CO_2 in solar system integrated with steam cycle.

Efficiency of an evacuated tube solar collector in which CO_2 used as a working fluid, has theoretically and experimentally investigated by Zhang and Yamaguchi [21]. Different types of energy sources (nuclear, solar, geothermal) were tested by the researchers [22] at Sandia National Laboratories to examine Brayton cycles application with S-CO_2 as a working fluid. Iverson et al [23] studied about fluctuating effect of solar energy input to S-CO_2 split flow recompression Brayton system. By dividing the heat input to two different percentages (50% & 100 %) for short time periods, they investigated the impact of these changes on power conditions. A

parabolic trough collector was also used to power the S-CO_2 cycle and developed by Singh et al [24]. He suggested that a well and accurate control system was mandatory for maintaining supercritical conditions of CO_2. Behavior of transcritical and supercritical CO_2 for solar thermal power applications were studied by Chacartegui et al [25] with consideration of three different types of S-CO_2 cycles. Five various S-CO_2 Brayton cycles were integrated with solar power tower system and compared thermodynamically by Sulaiman and Atif [26]. They investigated the system performance for three months (March, June and December) and concluded that the maximum overall efficiency was associated with recompression Brayton cycle (40 %) at June noon time.

To the best of our knowledge many researchers investigated on S-CO_2 Brayton cycles integrated with central receiver system and few researchers have been done on parabolic trough solar collectors incorporated with S-CO_2 cycles. However, this study attempts to understand the interaction between parabolic dish solar systems integrated with S-CO_2 Brayton cycles. The main aim of current research is to model a parabolic dish system and by using these modeling results to investigate the efficiency of the S-CO_2 Brayton cycles with and without reheat. This study focuses on the relation between rate of heat generation by the parabolic dish and the net power generated from both of the above mentioned S-CO_2 cycles.

Chapter 3

SYSTEMS DESCRIPTION

This section describes the two different classes of Brayton cycle, although there are many types of Brayton cycle such as, regenerative closed loop, pre-compression closed loop, split expansion, partial cooling with intercooling and recompression with reheat Brayton cycle. Due to the highest cycle efficiency and advancement in terms of different components, the recompression cycle is selected for the study. Furthermore, two recuperators are used with recompression cycle that eliminate the pinch point problem.

3.1 Simple Brayton Cycle

The simple Brayton cycle consists of only four components, compressor, combustion chamber, turbine and a heat exchanger as shown in Figure 3.1. The main compressor raises the pressure and temperature of the working fluid by compressing and then directing it to the combustion chamber in which fuel is burnt at constant pressure. After the combustion chamber this elevated temperature working fluid moves towards the turbine. It leaves the turbine by expanding to the atmospheric pressure, as a result it generates useful network output. Moreover, after the expansion process, the resulting gas rejects heat to the atmosphere.

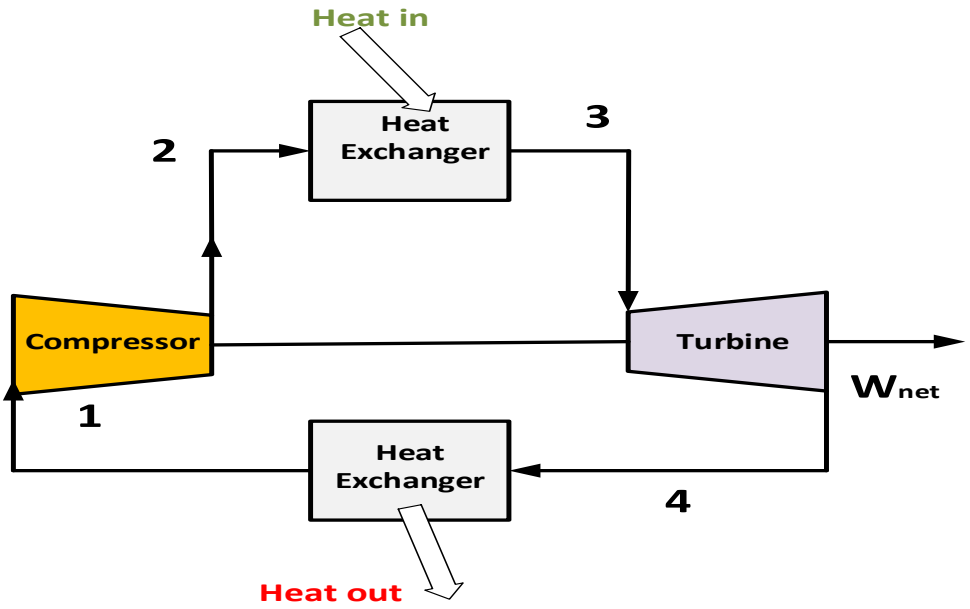

Figure 3.1: Simple Closed Gas Turbine Cycle

3.2 Advanced Brayton Cycle

The exhaust gas leaving the turbine usually has sufficient higher temperature as compared to the compressor outlet temperature. Therefore a regenerator or recuperator has an essential value to integrate with the closed loop Brayton cycle. Hot exhaust gases leaving the turbine can be regenerated so that it can exchange heat to the compressor exhaust gas. In this way a part of the heat of the exhaust gas (which is normally rejected to the surroundings) as mention by [5], can be utilized to preheat the gas entering the combustion chamber. Finally, heat input is reduced for the same turbine work. Intercooling, regeneration and reheating are also used to enhance the efficiency and performance of the closed loop Brayton Cycle. The network output of the turbine is basically the difference of the turbine work and compressor work which can be greater by reducing the compressor work (by increasing the number of stages using multi compressors) or by expanding the gas between two turbines (multistage expansion) with reheating. Such a system is presented in Figure 3.2.

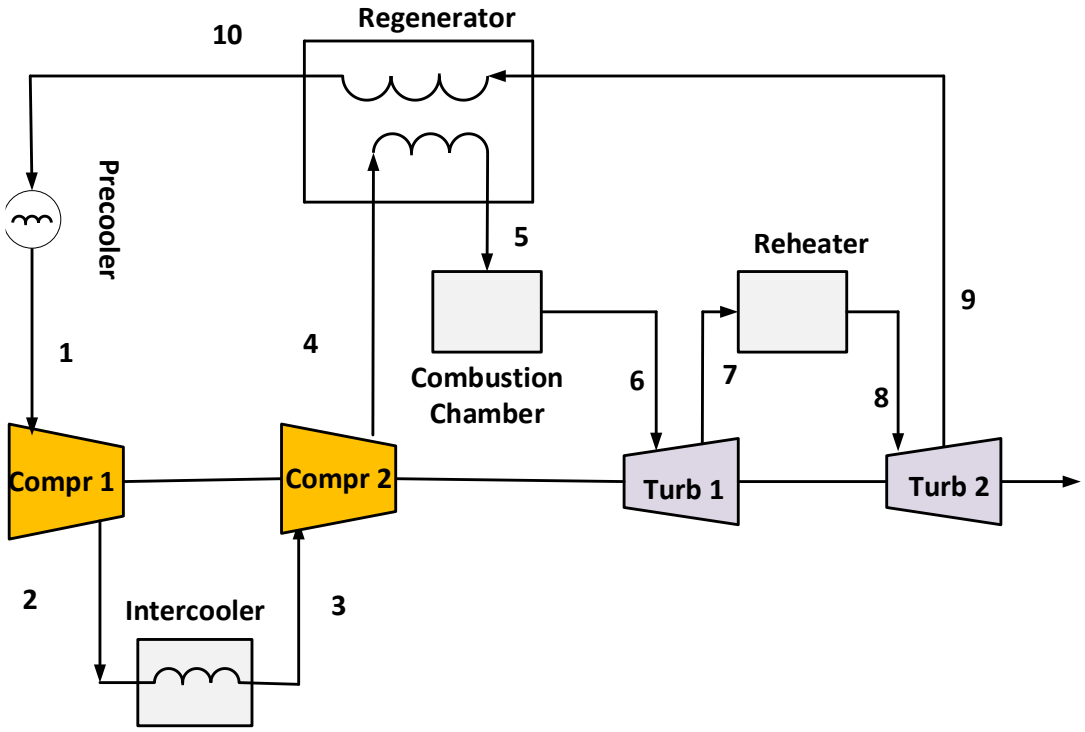

Figure 3.2: Recompression Gas-Turbine Cycle with Intercooling, Regenerative and Two-stage Expansion.

3.3 Parabolic Dish Solar Collector System (PDSC)

Nowadays parabolic dish systems have received attention due to their higher concentration ratio compared to the parabolic trough systems as stated by Kalogirou [6]. This system employs mirrors reflectors aligned on a dish shape that intensify the solar radiation on the focal point where the receiver is placed. The receiver is designed to absorb the incoming heat which can be used further in the power generation process [7]. Figure 3.3 shows the schematic of parabolic dish system. The receiver can be a cylindrical receiver, cavity receiver and drive a micro gas turbine or a Stirling engine. The initial cost of dish system is relatively higher than the trough system and the storage ability is less compared to the trough system.

The apparent shape of dish system is similar to the satellite TV or dish radar. The solar concentrator is a vital part or component of solar dish system. Dual-axis tracking

system is also used in this system to track the sun path and their concentration ratios are usually in the range of 600-2000 [6]. Moreover, they are capable of achieving a temperature of more than 1500 °C.

Table 3.1: Characteristics of various CSP technologies [2]

Parameters	**Parabolic Trough**	**Solar Tower**	**Linear Fresnal**	**Parabolic Dish**
Operating Temp. (°C)	350-550	250-565	390	550-750
Efficiency (%)	14/16	15/19	11/13	25/30
Optical efficiency	H	M	L	V.H
Con. ratio	70-80	1000	60-70	>1300
Cost	H	M	L	V.H

Parabolic dish system has an ability to achieve an efficiency of almost 31.25 % by converting solar radiation to power output, table 3.1 shows the performance matrix of different solar technologies.

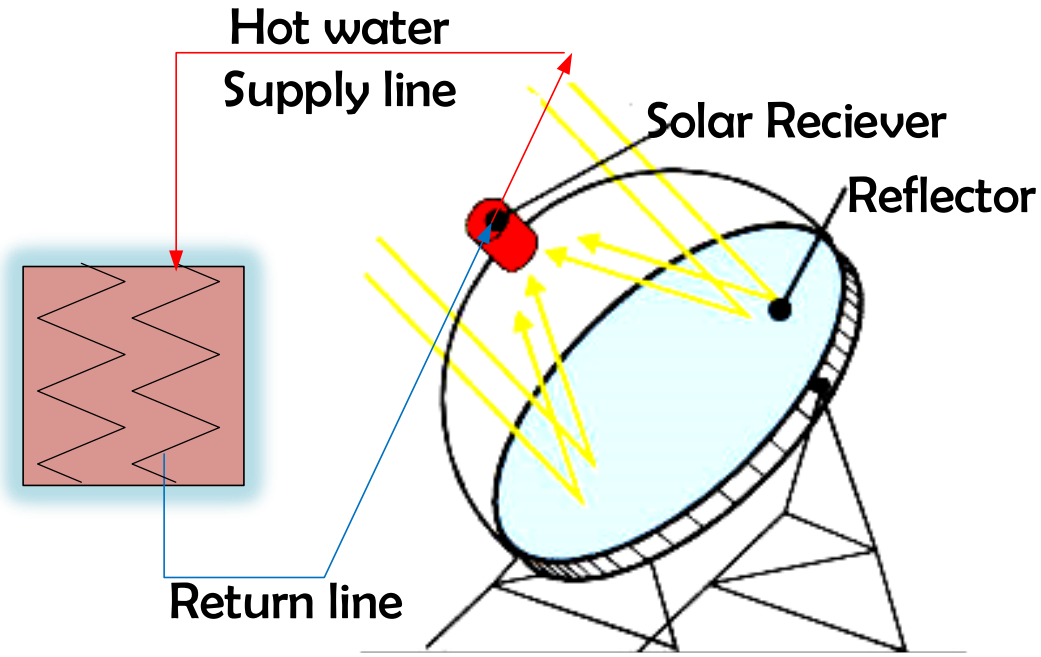

Figure 3.3: Schematic of the Parabolic Dish Solar Collector.

3.4 Integration of PDSC with Recompression S-CO_2 Brayton Cycle

This section of the thesis demonstrates the integration of the parabolic dish system with recompression with reheat and without reheat S-CO_2 Brayton cycles. Heat is generated by the PDSC system that will further utilize to run the turbines to accomplish the network output.

The thermo physical properties of carbon dioxide changes rapidly near critical conditions [15], the application of simple cycle configuration is reduced by temperature pinch point problems in the high temperature recuperator. This problem is caused because of the heat capacity rate difference of the fluid between cold side and hot side and explained by Turchi et al. [27]. Therefore, recompression Brayton cycles with two recuperators are suggested in this study. Schematic layout of the recompression without reheat system and its corresponding T-s diagrams is shown in Figure 3.4 and Figure 3.5. The efficiency of S-CO_2 system rises by using recompression version as heat rejected from the cycle is reduced by introducing another compressor (recompression compressor). The low pressure flow passes from low temperature regenerator (LTR) and divided into two streams at LTR exit (point 8). Main stream (1-x) ma becomes cool as it proceeds to pre-cooler through point (8a-1) and then through main compressor (1-2), its pressure increases and eventually enters into the LTR. The remaining low fraction stream with mass flow rate (x) ma passes through recompression compressor (8b) and meet the stream exiting LTR at state 3. Due to this split flow, cold fluid capacitance decreases so pinch point problems will be avoided. Before getting thermal heat from solar receiver, the main stream is heated through HTR and after the solar receiver it passes through the turbine at state 5. It is

important to concentrate that stream (8b) has non-zero flow and due to this, there is different mass flow rate for streams in LTR. Stream 7 has higher mass flow rate than that of stream 2. Furthermore, pressure of stream 7 is less than that of stream 2. Parabolic dish collector system (solar receiver) provides thermal heat to the Brayton cycles through heater and reheater. Hot water leaving the receiver enters into the heat exchanger at point 10 and after exchanging heat with the S-CO_2 cycle it comes back to the receiver collector via point 9. The outlet temperature of the fluid circulating in the collector loop is high enough to energize the S-CO_2 in the Brayton cycle. This heat energy is used to power the turbines to produce work output. Figure 3.2 illustrates the T-s sketch of the above mentioned system, which indicates that the turbine inlet temperature must be above than the 823 K, otherwise the system will not be capable of generating its required outputs.

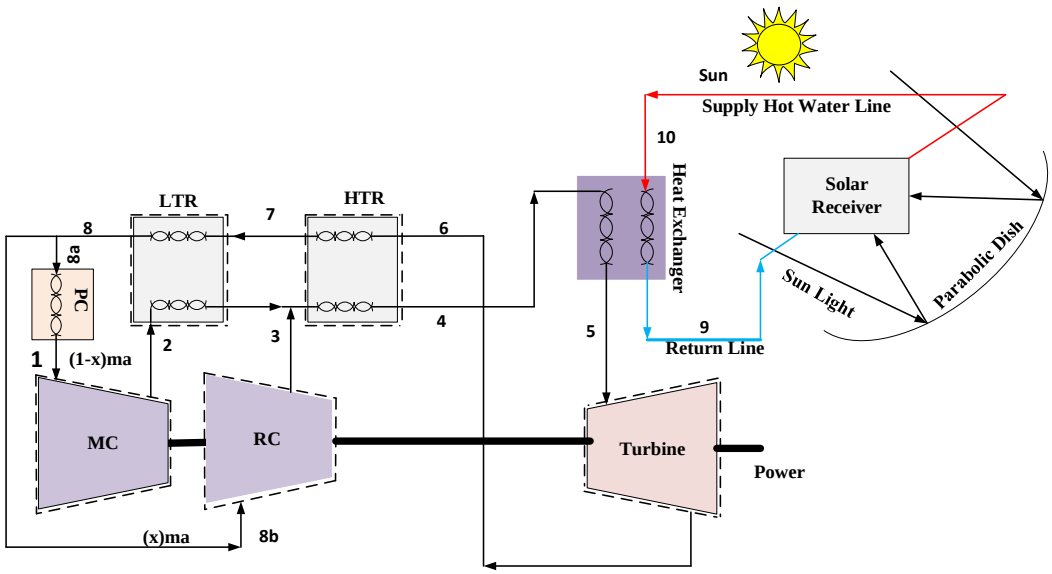

Figure 3.4: Schematic of the Suggested Solar-driven S-CO_2 Recompression Without Reheat Brayton Cycle

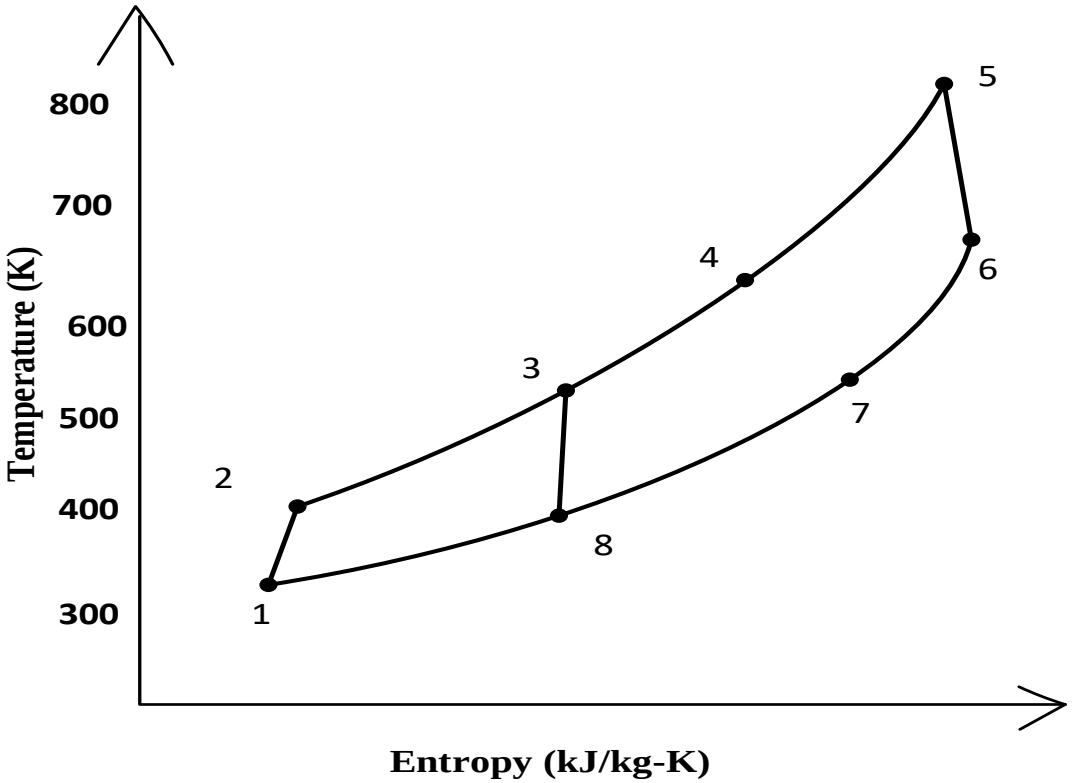

Figure 3.5: T-s Diagram of Recompression without Reheat S-CO_2 Brayton Cycle

All other steps used in recompression with reheat system are identical to the already described system but the reheat system applies two stage turbine with a reheater between the turbines shown by Figure 3.6,whereas, T-s diagram is shown in Figure 3.7. This modification improves the efficiency as well as the performance of the entire system.

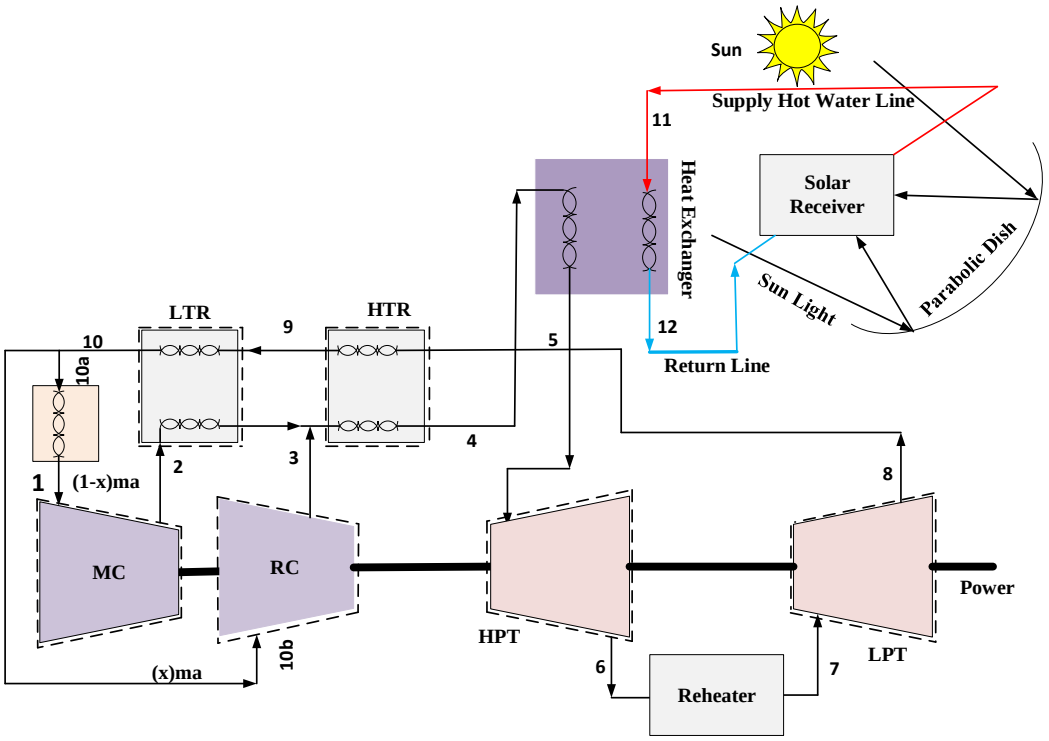

Figure 3.6: Schematic of the Proposed Solar-driven S-CO_2 Recompression with Reheat Brayton cycle

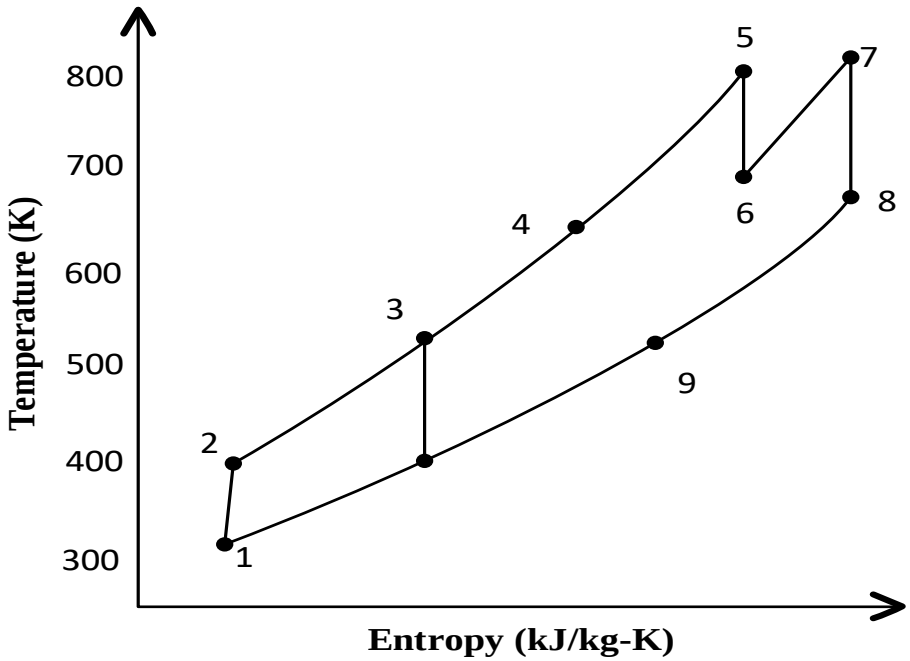

Figure 3.7: T-s diagram of recompression with reheat S-CO_2 Brayton cycle

Chapter 4

METHODOLOGY

4.1 Mathematical Modeling and Simulations

The following section of the dissertation provides detail about the mathematical modeling and the simulation of the individual systems and their integration. In addition, the methodology which analyzes the systems configuration to fulfill the proposed project requirements will be discussed.

Engineering equation solver (EES) [28] is employed for the assessment of mathematical modeling of the PDSC and S-CO_2 cycles. EES has the ability of solving simultaneously several complex linear and non-linear engineering equations while conducting the parametric study. Furthermore, it has built in thermodynamic properties and it eliminates iterative problem solving. The input data which is used to model the S-CO_2 Brayton cycle is listed in Table 4.1.

Main steps will be followed to achieve the objectives are:

1. Modelling and simulation of parabolic dish system and to evaluate its heat production rate, energetic and exergetic efficiencies and available solar exergy:
2. Simulation of recompression S-CO_2 cycle with reheat and without reheat including assessment of both systems for their further performance:

3. Integration of the PDSC with both the systems and overall performance of the integrated systems are compared:

4. Validation of the simulated results with the already published data.

The configuration of both types of Brayton cycles are modeled in two parts by consideration of the energy, exergy and mass analysis using Engineering Equation Solver (EES). The first part includes the modeling of two types of S-CO_2 Brayton cycles. a) S-CO_2 recompression Brayton cycle without reheating, b) S-CO_2 recompression Brayton cycle with reheating. The second part of the modeling is related to the design of parabolic dish collector system and the integration of the solar system to the S-CO_2 Brayton systems.

The energy and mass balance of the heat exchangers and turbo machines (compressors & turbines), are conducted initially. The effectiveness of HTR and LTR is calculated by considering a temperature difference between hot and cold sides of the fluid (see Equation 4.3 for HTR and Equations 4.4 & 4.5 for LTR) [18]. Following assumptions are used in this simulation, which are taken from [27, 29].

4.1.1 Assumptions

Pressure drop in the pipes and heat exchangers is assumed to be negligible.

The heat transfer with ambient surroundings is negligible:

Processes in the compressors and turbines are considered adiabatic:

The system attain steady state condition:

Table 4.1: Input Operating and Design Parameters for S-CO_2 Brayton Cycles

Temperature at the main compressor inlet [18]	305 K
Pressure at the main compressor inlet [18]	7.6 MPa
Pressure at the compressor exit	20 MPa
Mass flow rate [24]	19.6 kg/s
Effectiveness of HTR [26]	0.85
Effectiveness of LTR	0.7
Compressors isentropic efficiencies [26]	0.8
Turbines isentropic efficiencies	0.9

4.2 Energy Analysis of S-CO_2 Brayton Cycles

In this section, S-CO_2 recompression cycle with reheat is considered. A similar analysis can be made for the cycle without reheat; only this time the reheat component is omitted.

Thermodynamic relations of both recuperators for reheat system (see Figure 3.6):

$$h_8 - h_9 = h_4 - h_3 \qquad \text{(For HTR)} \qquad (4.1)$$

$$(1 - x)(h_3 - h_2) = (h_9 - h_{10}) \qquad \text{(For LTR)} \qquad (4.2)$$

where h represents the specific enthalpy of fluid in kJ/kg and x denotes the recompressed mass fraction in kg/s, respectively.

Effectiveness of HTR can be calculated as:

$$\varepsilon_{HTR} = (T_8 - T_9)/(T_8 - T_3) \qquad (4.3)$$

If the heat capacity of low pressure fluid is greater than that of high pressure fluid, effectiveness of LTR is given by equation (4.4):

$$\varepsilon_{LTR} = (T_3 - T_2)/(T_9 - T_2) \tag{4.4}$$

For reverse case equation (4.5) will be used:

$$\varepsilon_{LTR} = (T_9 - T_{10})/(T_9 - T_2) \tag{4.5}$$

Thermal heat available at storage heat exchanger is given as:

$$\dot{Q}_u = \dot{m}(h_5 - h_4) + \dot{m}(h_7 - h_6) \quad \text{(RH)} \tag{4.6 a}$$

$$\dot{Q}_u = \dot{m}(h_5 - h_4) \quad \text{(NO RH)} \tag{4.6 b}$$

ṁ and $\dot{Q}_u$ denotes the mass flow rate of CO_2 and useful thermal energy, respectively:

Thermodynamic relations of other components can be expressed as:

Turbine power can be expressed as:

$$\dot{W}_{tur} = \dot{m}.(h_5 - h_6) \tag{4.7a}$$

$$\dot{W}_{tur} = \dot{m}.(h_5 - h_6) + \dot{m}.(h_7 - h_8) \tag{4.7b}$$

where Ẇ represents the available power in kW. The equation (4.7a) is used for without reheating system, whereas, the other one will be for reheating cycle.

For the main compressor, power input is given as:

$$\dot{W}_{mc} = \dot{m}(1 - x)(h_2 - h_1) \tag{4.8}$$

And for the second compressor, power input is:

$$\dot{W}_{recomp} = \dot{m}.x(h_3 - h_{10}) \tag{4.9}$$

The heat discarded at the pre cooler is:

$$\dot{Q}_{out} = \dot{m}.(1-x)(h_8 - h_1) \quad \text{(Without reheat)} \tag{4.10a}$$

$$\dot{Q}_{out} = \dot{m}.(1-x)(h_{10} - h_1) \quad \text{(With reheat)} \tag{4.10b}$$

Isentropic efficiencies of main compressor and re compressors can be defined as:

$$\eta_{mc} = \frac{h_{2s}-h_1}{h_2-h_1} \tag{4.11}$$

$$\eta_{rc} = \frac{h_{3s}-h_{10}}{h_3-h_{10}} \tag{4.12}$$

Isentropic efficiencies of both turbines can be calculated as:

$$\eta_{hpt} = \frac{h_5-h_6}{h_5-h_{6s}} \tag{4.13}$$

$$\eta_{lpt} = \frac{h_7-h_8}{h_7-h_{8s}} \tag{4.14}$$

Net work output from the Brayton cycle will be:

$$\dot{W}_{net} = \dot{W}_{tur} - \left(\dot{W}_{mc} + \dot{W}_{recomp}\right) \tag{4.15}$$

Thermal efficiency of both the cycles can be expressed as:

$$\eta_{th} = \dot{W}_{net}/\dot{Q}_u \tag{4.16}$$

4.3 Exergy Analysis of S-CO_2 Brayton Cycles

Exergy is also known as an availability and the maximum theoretical work obtained by the system and specified reference surroundings (environment). The second law analysis or exergy analysis allows to overcome many of the drawbacks of energy analysis. Exergy analysis depends upon second law of thermodynamics and is used to identify the reasons, positions and quantity of the system's process inefficiencies [30].

The exergy, exergy destruction of individual components and exergy efficiency of S-CO_2 Brayton cycle is assessed at all the relevant points and will be presented here.

Exergy at all points is calculated by $e_x = h - T_o.s$ [17] considering that both enthalpy and entropy are zero at dead state.

where e_x the specific exergy (kJ/kg) and s is stands for specific entropy (kJ/kg-K) and the specific exergy at the inlet of main compressor can be calculated as:

$$e_x = (1-x)(h_1 - h_0) - T_0.(s_1 - s_0) \tag{4.17}$$

Similarly, specific exergy at all other states can be determined using the same procedure. Furthermore, exergy destruction rate by different components can be expressed as:

$$\dot{\psi}_{des,pc} = \dot{m}(1-x)(X_{10} - X_1) \tag{4.18}$$

$$\dot{\psi}_{des,mc} = \dot{W}_{mc} - \dot{m}(1-x)(X_2 - X_1) \tag{4.19}$$

$$\dot{\psi}_{des,rc} = \dot{W}_{rc} - \dot{m}x(X_3 - X_{10}) \tag{4.20}$$

$$\dot{\psi}_{des,HTR} = \dot{m}(X_8 + X_3) - \dot{m}(X_9 + X_4) \tag{4.21}$$

$$\dot{\psi}_{des,LTR} = \dot{m}(X_9 - X_{10}) - \dot{m}.(1-x)(X_3 - X_2) \tag{4.22}$$

$$\dot{\psi}_{des,hpt} = (X_5 - X_6) - \dot{W}_{hpt} \tag{4.23}$$

$$\dot{\psi}_{des,lpt} = (X_7 - X_8) - \dot{W}_{lpt} \tag{4.24}$$

The second law efficiency of the Brayton cycle is:

$$\eta_X = \dot{W}_{net}/X_{in} \tag{4.25}$$

where $\dot{X}_{in}$ is the rate of exergy input to the cycle and is defined as [31]:

$$\dot{X}_{in} = \left(1 - \frac{T_0}{T_s}\right) . \dot{Q}_u \quad (4.26)$$

where T_s is the source temperature:

4.4 Solar Data and Location

Southern part of Pakistan has a very high solar radiation intensity, almost more than the 1000 W/m^2, specially Southern Punjab, Baluchistan and Sindh [32]. The current simulations were conducted by considering direct normal irradiation (DNI) for Bahawalpur. Latitude for the location is 29^o 25 / 5.0448 N while longitude is 71^o 40 / 14.4660 E [33]

4.5 Parabolic Dish Solar Collector (PDSC)

The Parabolic dish solar collector model is investigated by following the suitable mathematical relations and table 4.2 shows the input design parameters for parabolic dish system. The dish model used in current study has been taken from the system proposed by Lloyd C. Ngo [34]. Table 4.3 gives the detail comparison of different CSP technologies [2].

Table 4.2: Input Design Conditions for PDSC

Aperture area ($\boldsymbol{A_a}$)	10.46 m^2
Receiver area ($\boldsymbol{A_r}$)	0.0316 m^2
Ambient pressure	100 kPa [10]
Ambient temperature	300 K [34]
Inlet temperature	350 K [10]
DNI	1000 W/m^2
Mass flow rate	0.1 kg/s
Optical efficiency	0.85 [34]

4.5.1 Energy Analysis of PDSC

The energy efficiency of the collector can be defined by the relation:

$$\eta_{en} = \frac{\dot{Q}_u}{Q_{sun}} \tag{4.27}$$

where Q_{sun} is the net heat available from the sun which is proportional to the area of the aperture (A_a) and G_b is the incident solar radiation per unit area of concentrator:

$$Q_{sun} = G_b A_a \tag{4.28}$$

The useful energy Q_u available by solar system can be defined as:

$$\dot{Q}_u = \dot{Q}_r - \dot{Q}_l \tag{4.29}$$

$\dot{Q}_r$ is the solar energy radiation falling on the receiver and $\dot{Q}_l$ is the heat loss from the receiver and is obtained as:

$$\dot{Q}_l = U_L A_r (T_r - T_0) \tag{4.30}$$

Where U_L represents the coefficient of overall heat transfer, which comes by the summation of conduction, convection and radiation heat losses of the solar collector and A_r is the receiver area.

The heat gain is calculated by taking the fluid temperature difference also:

$$\dot{Q}_u = \dot{m}\, C_P (\, T_{out} - T_{in}\,) \tag{4.31}$$

The actual heat available from dish solar system can also be calculated by applying famous Hottel-Whillier equation [34]:

$$\dot{Q}_u = A_a F_R \left(S - \frac{A_r}{A_a} U_L (T_{in} - T_0) \right) \tag{4.32}$$

where S denotes the absorbed radiation ($S = \eta_0 G_b$) and η_0 is the optical efficiency or thermal performance of the parabolic dish receiver ($\eta_0 = 0.85$) as taken from [35].

Heat removal factor F_R can be expressed as [6]:

$$F_R = \frac{\dot{m} C_P}{A_r U_L}\left[1 - \exp\left(\frac{A_r U_L F_1}{\dot{m}\, C_P}\right)\right] \tag{4.33}$$

F_1, the ratio between U_L and U_0 is the overall heat loss coefficient [6]:

The concentration ratio is given by the relation:

$$C = \frac{A_a}{A_r} \tag{4.34}$$

Aperture and receiver area of PD concentrator can be found as:

$$A_a = \pi R^2 \tag{4.35}$$

$$A_r = \frac{\pi d^2}{4} \tag{4.36}$$

R is the radius of the aperture and d is the diameter of the receiver.

Overall energetic efficiency of integrated system can be determined as:

$$\eta_{en,ov} = \dot{W}_{net}/\dot{Q}_{solar} \tag{4.37}$$

Where $\dot{Q}_{solar}$ is the heat rate of the sun radiation and given by:

$$\dot{Q}_{solar} = \frac{F_R A_a S}{1000} \tag{4.38}$$

4.5.2 Exergy Analysis of PDSC

The maximum possible work potential that is produced by parabolic dish collector can be find through exergy analysis. To calculate the total exergy of the dish receiver, it is necessary to find out exergy in and exergy out from the receiver:

$$\dot{X}_{in} = \dot{m}_r . C_p\left(T_i - T_o - T_o . ln(T_i - T_o)\right) \tag{4.39}$$

$$\dot{X}_{out} = \dot{m}_r . C_p\left(T_{out} - T_o - T_o . ln(T_{out} - T_o)\right) \tag{4.40}$$

$$\dot{X}_{tot} = \dot{X}_{out} - \dot{X}_{in} \tag{4.41}$$

The rate of total exergy content of solar is estimated by using Patella's approach [36] and is given as:

$$\dot{X}_{solar} = G_b . A_a . \eta_{pet} \tag{4.42}$$

where η_{pet} is the Patella's efficiency.:

$$\eta_{pet} = 1 - \frac{4T_0}{3T_{su}} + \frac{1}{3}\left(\frac{T_0}{T_{su}}\right)^4 \tag{4.43}$$

X_{solar} can be found as:

$$\dot{X}_{solar} = \left(1 - \frac{T_0}{T_{sun}}\right) . \dot{Q}_{solar} \tag{4.44}$$

Finally, exergy efficiency of the PD solar collector and integrated system can be analyzed as, respectively:

$$\eta_{X,PDSC} = \frac{\dot{X}_{tot}}{\dot{X}_{solar}} \tag{4.44}$$

$$\eta_{X,ov} = \frac{\dot{W}_{net}}{\dot{X}_{solar}} \tag{4.45}$$

Chapter 5

RESULTS AND DISCUSSION

This part of the study illustrates in detail the simulation and modelling results of the solar collector system, S-CO_2 Brayton cycles, their integration with the PDSC and comparison of outputs between both integrated systems as well as validation of results with the already published data.

The current study is based on simulations and modelling instead of the experimentation. Two different types of closed loop S-CO_2 Brayton cycles (recompression with reheat and recompression without reheat) are studied thoroughly. In addition, these cycles are integrated with parabolic dish collector system. Both of the integrated systems are compared by changing the operating parameters (DNI, mass flow rate in to the receiver, inlet temperature of the receiver, ambient temperature, pressure ratio, minimum cycle temperature) and their effect on the performance parameters (rate of heat generated, network output and integrated system energy and exergy efficiencies) are investigated.

5.1 Effect of Mass Flow Rate

The mass flow rate of fluid in solar collector has a positive impact on the performance of the system. The convection heat transfer coefficient is directly associated with the performance of the solar system as it varies with mass flow rate, giving better productivity.

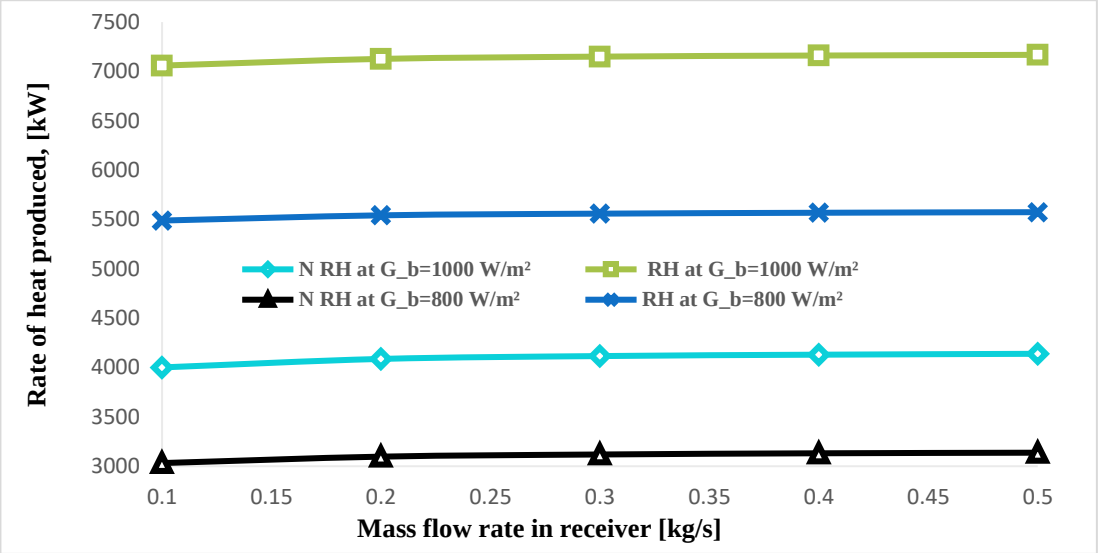

Figure 5.1: Influence of Mass Flow Rate on Heat Production Rate at Different Solar Irradiations

Greater mass flow rate of the heat transfer fluid in solar collector gives maximum outlet temperature of the collector which will contribute slightly more rate of heat produced as relation given in equation 4.31. As a result, network output and efficiency increases. Increasing the mass flow rate from 0.1 kg/s to 0.5 kg/s, rate of heat produced increases marginally from 5.489 MW to almost 5.574 MW when DNI is 800W/m^2 and 7.059 MW to 7.168 MW at DNI 1000W/m^2 for reheat system**,** respectively as depicted in Figure 5.1. Increase in heat production rate for without reheat system is increased between 3.032 MW and 3.137 MW for DNI 800W/m^2**,** whereas, increases from 4.001 MW to 4.139 MW when the solar irradiation is 1000W/m^2, accordingly.

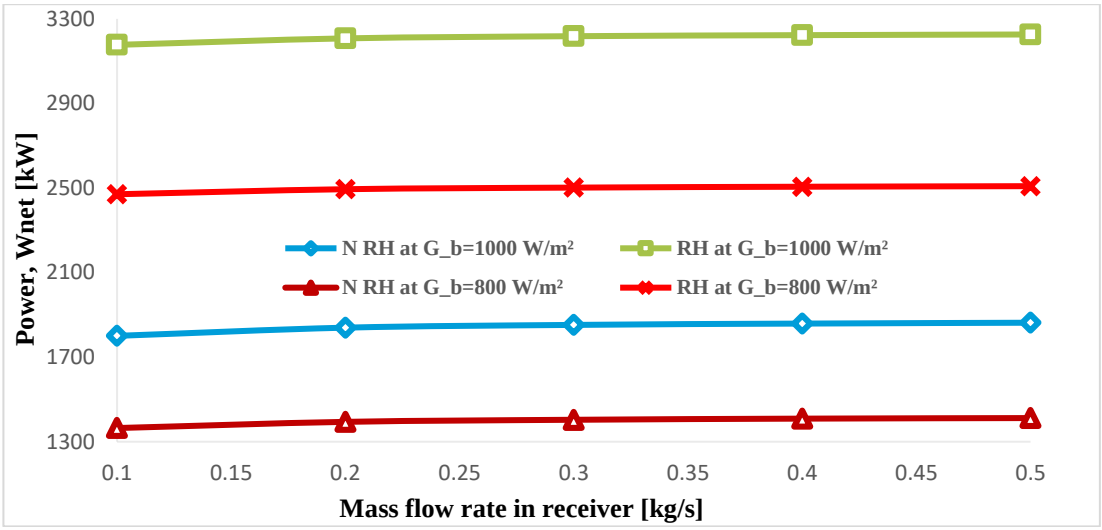

Figure 5.2: Effect of Mass Flow Rate on Net Power Output at Different Solar Irradiations

Figure 5.2 shows the effect of mass flow rate on network produced by integrated supercritical carbon dioxide Brayton cycles at different solar irradiations. Recompression with reheat cycle generates more power output significantly as compared to recompression without reheat cycle. For reheat cycle, the mass flow varies from 0.1 kg/s to 0.5 kg/s, the net power output increases from approximately 2.4704 MW to near about 2.5086 MW when solar radiation is 800 W/m^2. However, for no reheat cycle, work output is increased from 1.3645 MW – 1.4118 MW. Furthermore, when the solar intensity increases from 800 W/m^2 to 1000 W/m^2, reheat system generates power between 3.177 MW to 3.226 MW, however, without reheat system gives output between 1.800 MW to 1.862 MW, respectively. These outputs clearly show that reheating increases work out put as well as the performance of the system considerably. Increasing the mass flow rate enhances the heat produced rate slightly that is directly related to turbine work output. As the network output of the Brayton cycle is the turbine work minus the compressor work and it will be greater by increasing the turbine work (more than one turbine). Due to this reason reheat cycle gives more work as compared to the no reheat cycle.

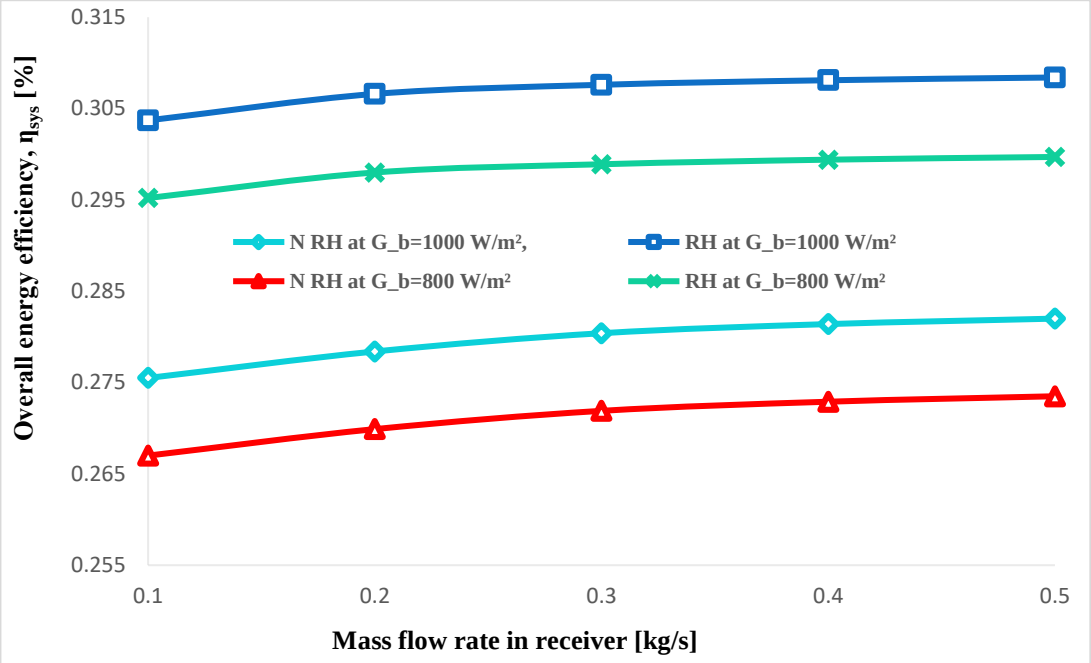

Figure 5.3: Effect of Mass Flow Rate on Integrated System Efficiency at Different Solar Irradiations

Overall energy efficiency of the integrated system relies on network output and heat rate of solar (see Equation 4.38). Figure 5.3 shows the impact of the rate of mass flow in solar collector on integrated energy efficiency of the systems. Likewise the heat produced rate and the network, energy efficiency of the integrated system will be higher for reheat cycle rather than without reheat cycle. When solar intensity is 1000 W/m^2, efficiency of reheat system increases from 30.37% to 30.84%. However, the efficiency of other system increases from 27.50% to 28.20% approximately. The same trend is found for both the systems at the other value of solar intensity. The reheating improves the overall energy efficiency up to 10.43%.

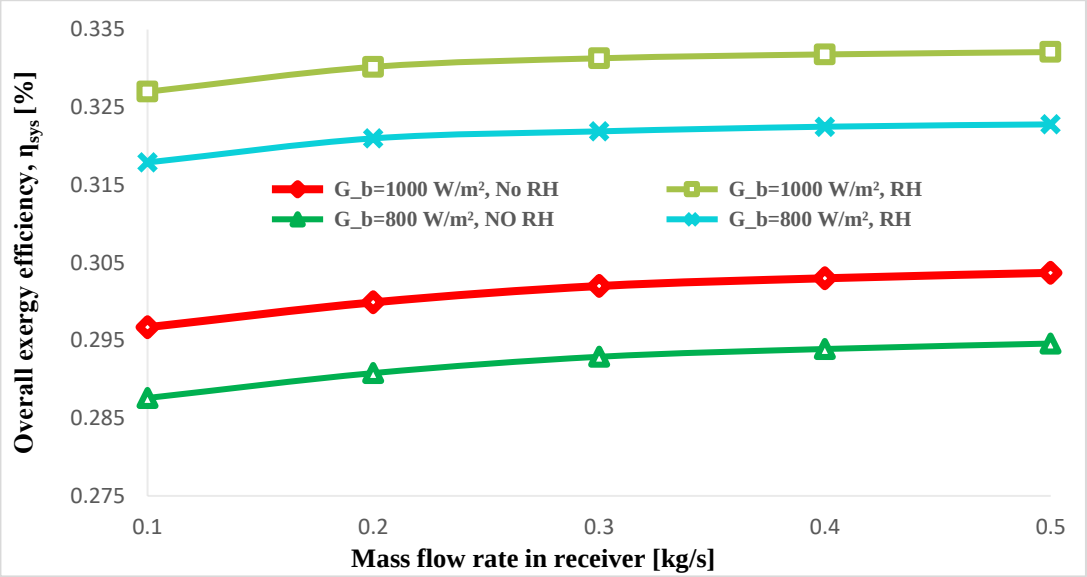

Figure 5.4: Influence of the Receiver Mass Flow Rate on Overall Exergetic Efficiency at Different Solar Irradiations

The overall exergy efficiency of the integrated system is related to exergy of the solar radiations (available rate of solar exergy) (see Equation 4.42). These values are more than the energy efficiency values exergy represents total possible availability of the work as given by Figure 5.4 but it follows the same directions of overall energy efficiency and increases steadily. For reheat cycle with 1000 W/m^2, exergy efficiency increases from almost 32.70 % to 33.21 % and for second system exergy efficiency approaches between 29.67 % and 30.37 % nearly.

5.2 Effect of Solar Irradiation

Solar intensity or solar beam radiation is the most important inlet parameter which influences the performance of the solar collectors as well as the efficiency of whole system. The countries with the more solar radiation, are suitable and economical for the investment of solar thermal power plants. This is basically the energy transferred of the heat transfer fluid that is circulating in the collector loop. By increasing the solar radiation, the outlet temperature of the receiver is enhanced linearly.

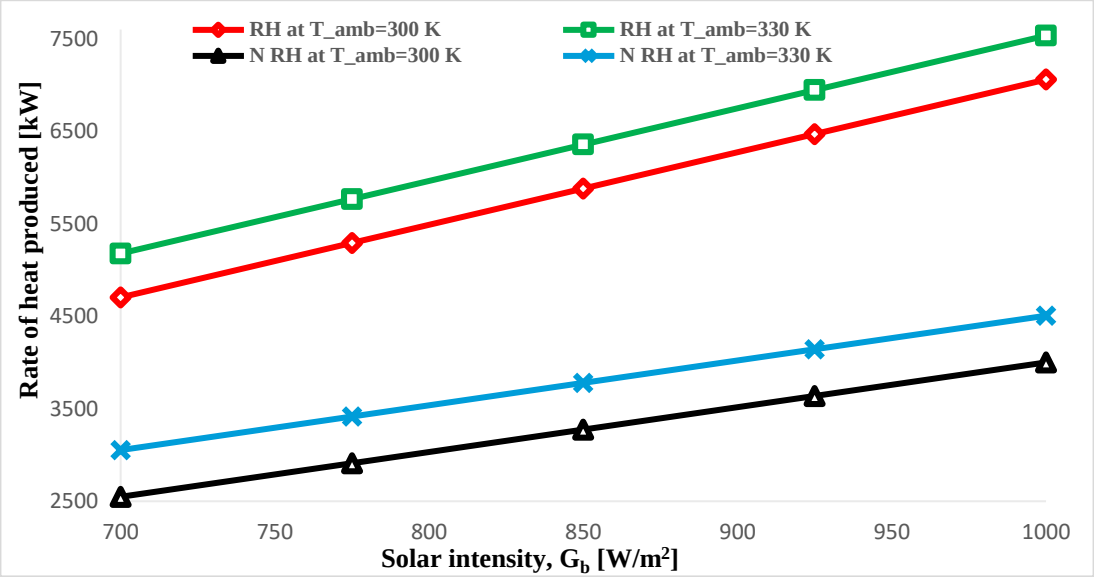

Figure 5.5: Impact of Solar Irradiation on Heat Production Rate at Various Ambient Temperatures

Figure 5.5 and Fig 5.6 provide information related to the impact of solar intensity on the rate of produced heat and the network output by both of the integrated systems at different ambient temperatures. Solar radiation varies from 700 W/m^2 to 1000 W/m^2, as a result, the rate of heat produced of reheat system will increase nearly from 5.179MW to almost 7.534 MW when ambient temperature is 330 K, while the other system is produced heat from 3.053 MW to 4.506 MW almost. For other value of ambient temperature, heat generation rate is slightly less but following the same footsteps.

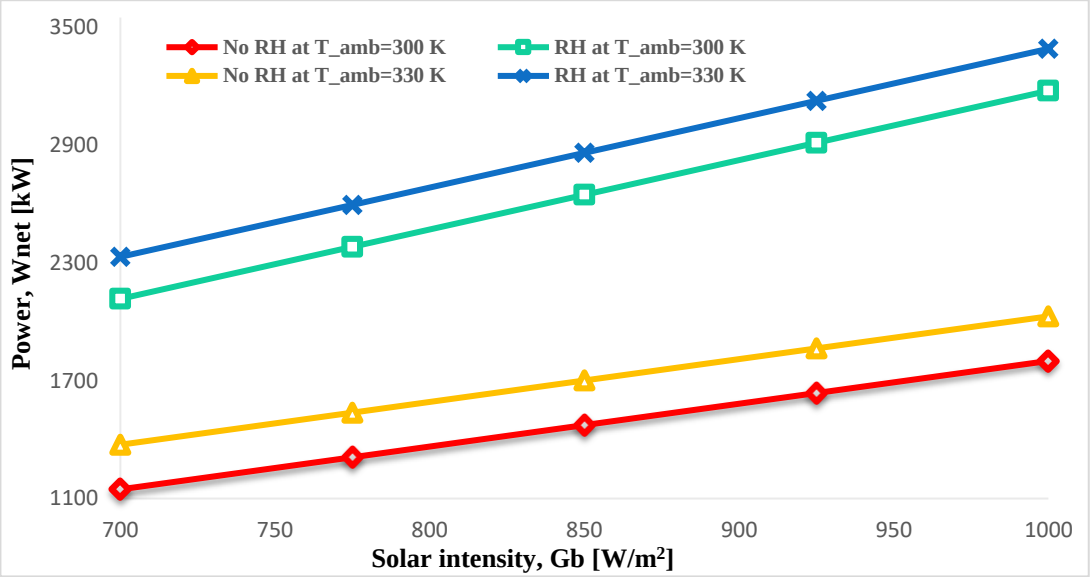

Figure 5.6: Effect of Solar Intensity on Power Output at Various Ambient Temperatures

By changing the beam radiations between the specified range, recompression with reheat system produces significantly more network output as compared to the other system. Power linearly increases from 2.330 MW to 3.390 MW**,** approximately, when ambient temperature is 330 K for reheat cycle. However, for no reheat system the net power output rises from 1.374 MW to 2.027 MW for the same value of ambient temperature.

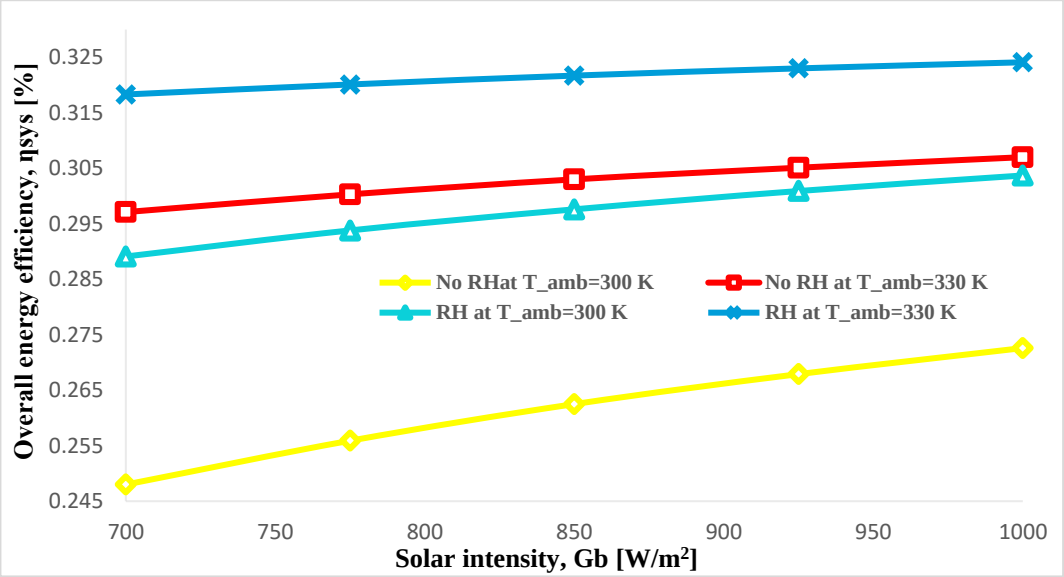

Figure 5.7: Influence of DNI on Overall Energetic Efficiency of the Systems

Solar intensity has major effect on the overall energy and exergy efficiency of the integrated systems whether it is reheat or without reheat system as shown in Figure 5.7 and Figure 5.8. The reheat integrated system has an overall energy efficiency between 28.91% and 30.37 % at ambient temperature of 300 K. However, the latter system also shows a promising reflection between 24.80% and 27.26 % for the same conditions, showing that the reheating improves overall energy efficiency up to 11.39 per cent, approximately. When the ambient temperature is 330 K, this performance parameter has slightly higher values between 31.83 % and 32.41 % for reheat system and from 29.71 % to 30.70 % for without reheat system. The overall second law efficiency has greater values than the energetic efficiency values. For reheating system, the exergy efficiency varies from 34.54 % to 35.18 % at an ambient temperature of 330 K and the second system has overall exergy between 32.27 % and 33.32 % for the same ambient temperature. Furthermore, at other value of ambient temperature, efficiency of both systems increase linearly but below for the values of 330 K. The variation in efficiencies is quite smoothly for higher ambient temperatures (330 K), whereas, change in efficiencies is little bit dramatically when ambient temperature is 300 K for

both the integrated systems. The reason behind is due to the more temperature difference when ambient temperature will be low, which gives more heat production rate as given by equation 4.32.

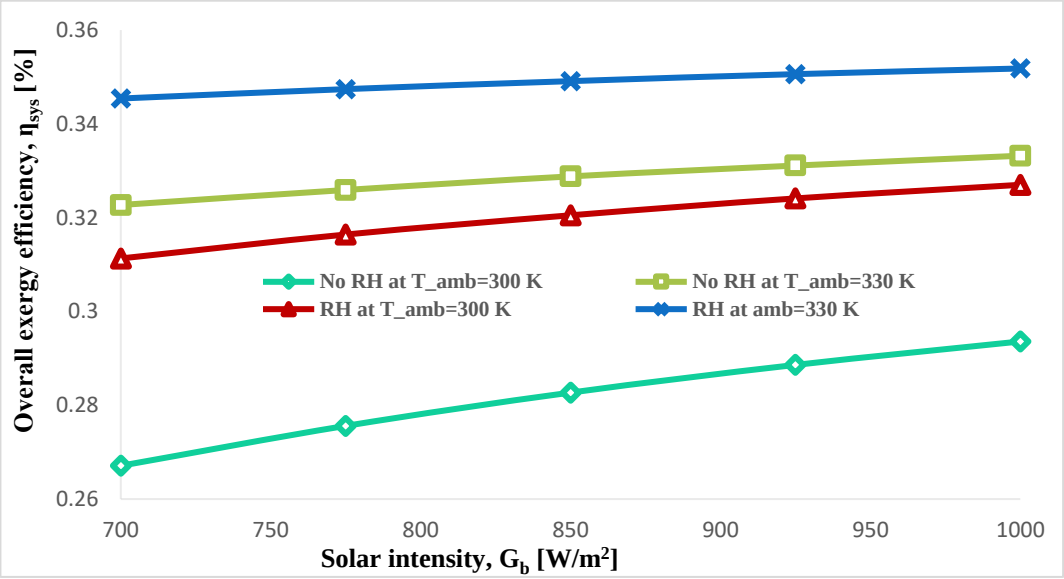

Figure 5.8: Effect of Solar Intensity on Overall Exergy Efficiency of the System

5.3 Influence of Ambient Temperature

The warm ambient surrounding plays an essential role to increase the performance of solar collectors and it is the foremost input parameter which affects the performance of the solar thermal plants. When the ambient temperature is high, solar collector receives more energy results in higher outlet temperature. Higher outlet temperature gives the higher rate of heat production and ultimately more network output. The performance of the system is improved finally.

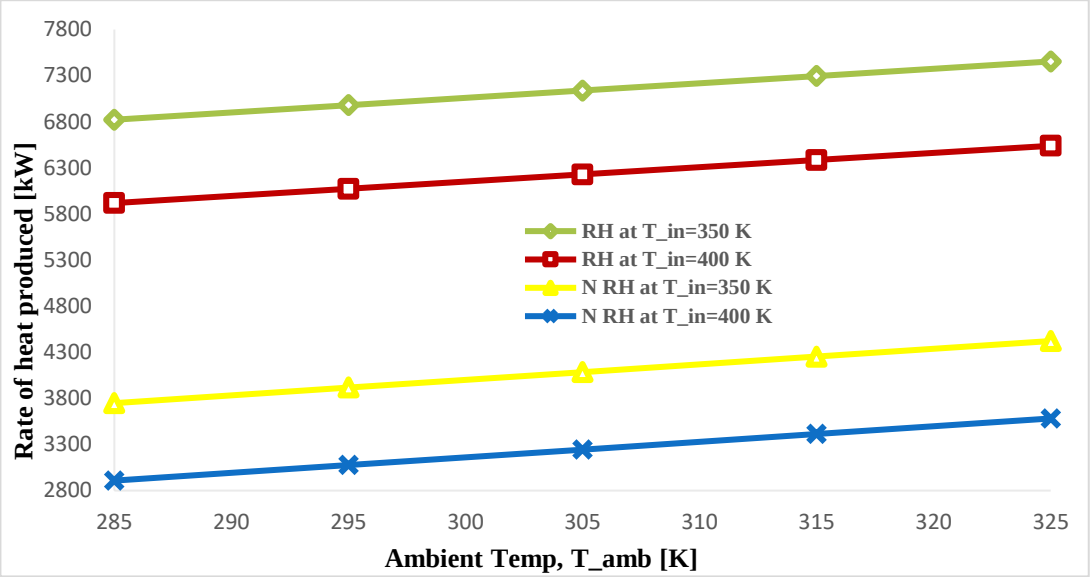

Figure 5.9: Effect of Ambient Temperature on Heat Production Rate at Different Inlet Temperatures

Figure 5.9 shows the effect of ambient temperature on rate of heat produced at two different inlet temperatures. As ambient temperature is increasing from 285 K to 325 K of reheat system, heat generation rate will gradually enhance between 6.822 MW to 7.454 MW approximately, while the system without reheat produces heat from 3.748 MW to 4.442 MW, accordingly, for inlet temperature of 350 K. For higher values of inlet temperature, system produces less heat as the difference between outlet temperature and inlet temperature is reduced.

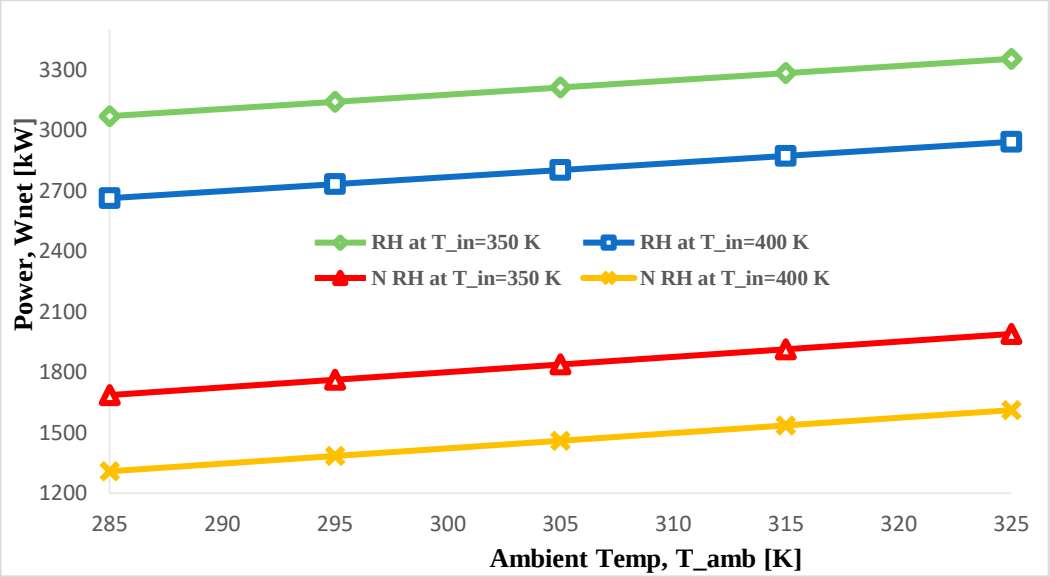

Figure 5.10: Effect of Ambient Temperature on Power Output at Different Inlet Temperatures

As ambient temperature varies, network output also increases similarly to the heat production rate. Recompression with reheat Brayton system generates substantial more work as compared to the recompression without reheat system. When inlet temperature is 350 K, reheat integrated system generates almost 3.070 MW to 3.353 MW, whereas, the other system gives 1.686 MW to 1.990 MW network. By increasing the inlet temperature up to 400 K, the values of network output lies in the range of 2.663 MW to 2.942 MW for reheat system and 1.308 MW to 1.612 MW for without reheat system, approximately and is given by Figure 5.10.

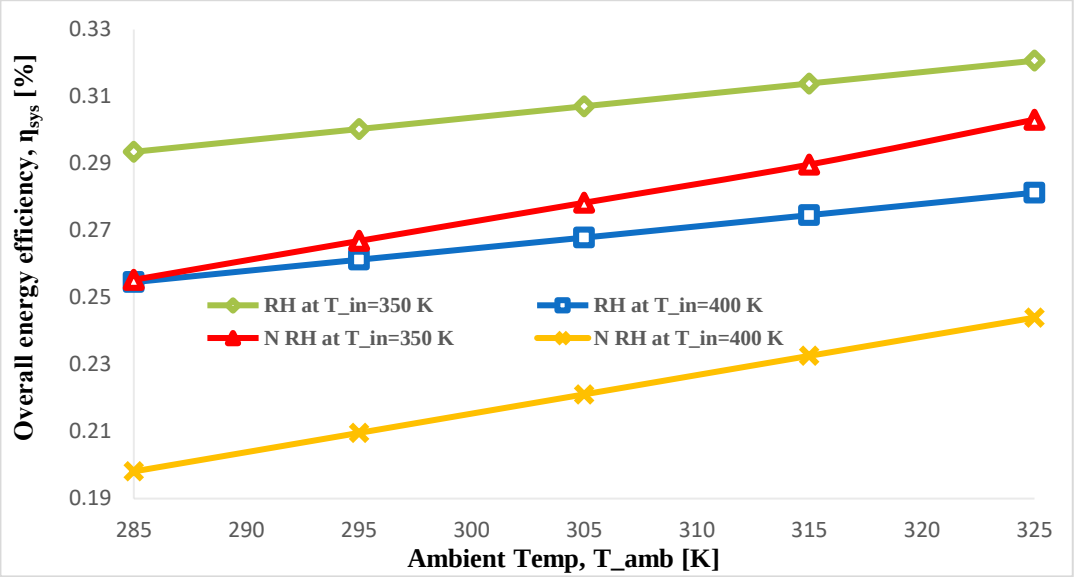

Figure 5.11: Effect of Ambient Temperature on Overall Energy Efficiency of the Systems

Overall energy and exergy efficiency of the integrated system is directly related to the ambient temperature. For reheat cycle at inlet temperature of 350 K, energy efficiency increases linearly from 29.35 % to 32.07 % and without reheat system it increases from 25.53 % to 30.31 %. However, when the inlet temperature is 400 K, efficiency will be less for both the systems as compared to the lower inlet temperature values as shown in Figure 5.11.

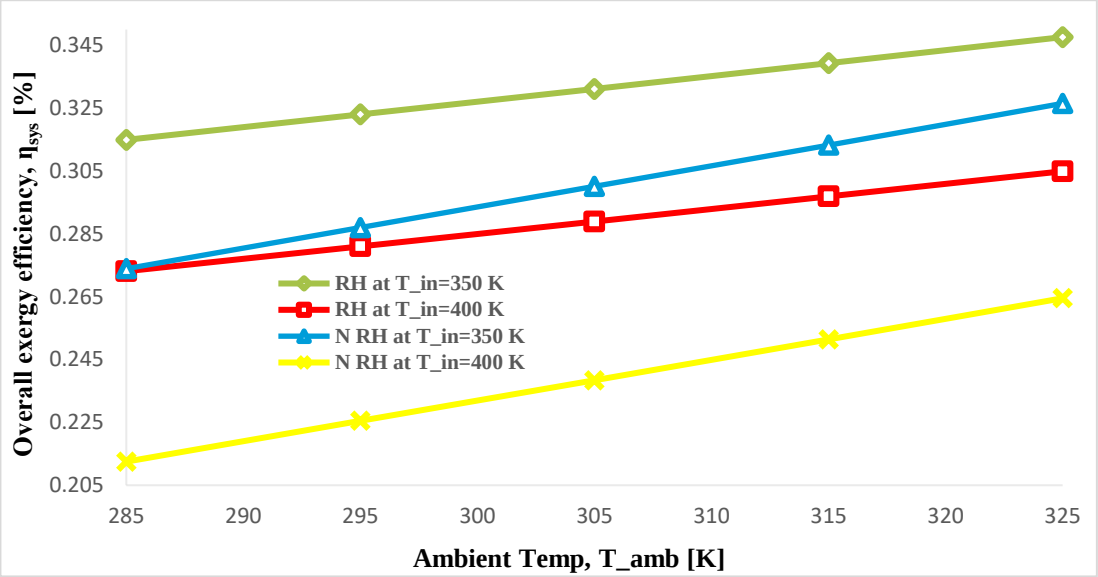

Figure 5.12: Effect of Ambient Temperature on Overall Exergy Efficiency of System

Overall exergy efficiency of both systems is plotted against ambient temperature in Figure 5.12 and it depicts similar behavior that is described for overall energy efficiency in Figure 5.11. However, these values are greater than the integrated energy efficiency. By fixing the inlet temperature at 350 K, exergy efficiency of the reheating system rises linearly from 31.49% to 34.76%. Furthermore, integrated Brayton system without reheating has an overall exergy efficiency between 27.39 % and 32.65 %.

5.4 Effect of Inlet Temperature

Inlet temperature of the heat transfer fluid is another key parameter that changes the performance of the solar collectors as well as the whole integrated system. Figure 5.13 shows the relation of the heat production rate with the increase in receiver inlet temperature at different solar irradiations.

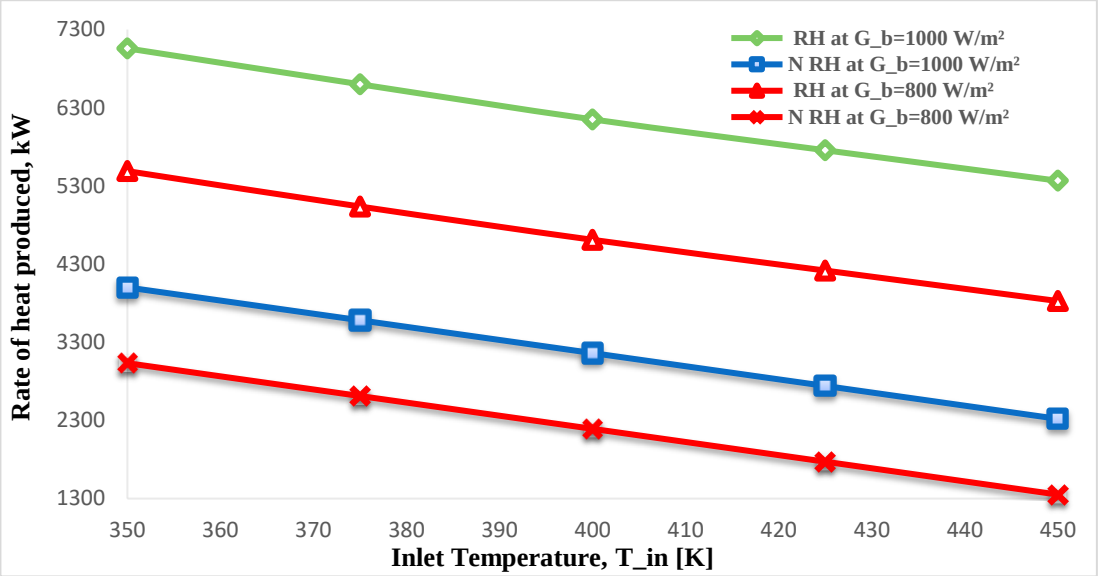

Figure 5.13: Effect of Inlet Temperature of Receiver on Rate of Heat Produced

By increasing the inlet temperature, the above said performance parameter is reduced for reheat and for without reheat integrated systems approximately from 7.059 MW to 5.366 MW for DNI 1000 W/m^2 and from 4.001 MW to 2.320 MW, respectively. This is due to the surface temperature of the absorber tube becomes greater when fluid inlet temperature rises. Therefore heat losses to the surrounding also enhances that lowers the rate of heat production, network output and efficiency as well. Net power generation by both the integrated systems are reduced from 3.177 MW to 2.415 MW for reheat system and 1.800 MW to 1.044 MW for without reheat system, respectively as inlet temperature increases from 350 K to 450nK at solar intensity of 1000 W/m^2. Figure 5.14 also shows the variation in power output for other value of DNI.

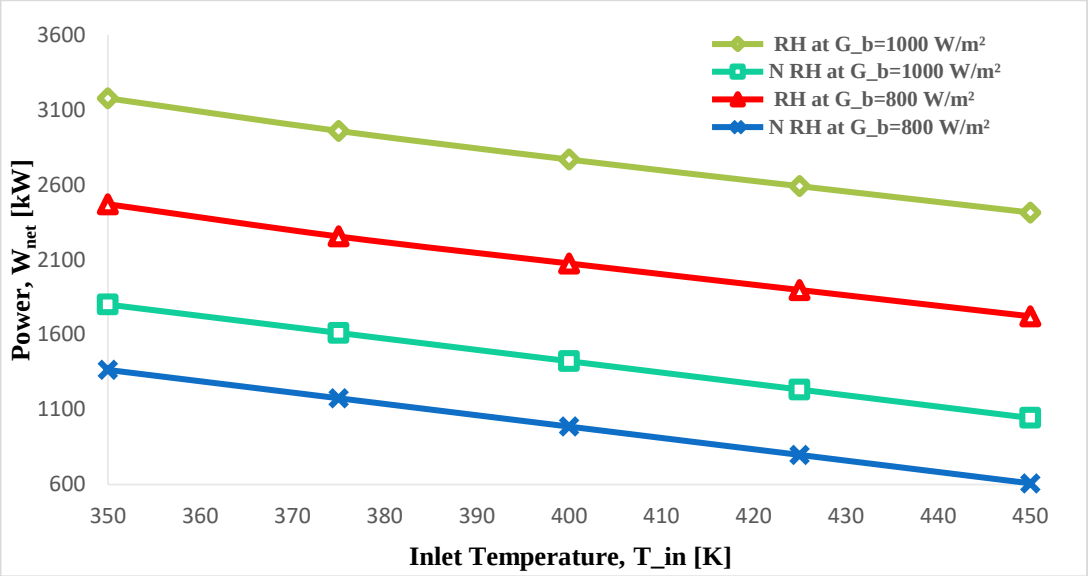

Figure 5.14: Effect of Inlet Temperature of Receiver on Net Power Output

The integrated energy efficiency of reheat system is reduced from 30.37% to 23.08%, while 27.26% to 15.80% degradation in energy efficiency is observed for without reheat system by varying the inlet temperature from 350 K to 450 K, shown in Figure 5.15. Furthermore, overall energy efficiency values for both the systems at DNI=800 W/m^2 is decreased in a similar pattern. Overall exergy efficiency of both of the systems follow the same guide line as illustrated for overall energy efficiency. Exergy efficiency reduces from 32.7 % to almost 24.86 % for reheat system with an outstanding difference of 11.37 % at DNI 1000 W/m^2 over the recompression without reheat system. The decrease in the overall exergy efficiency at other value of DNI is also plotted in Figure 5.16.

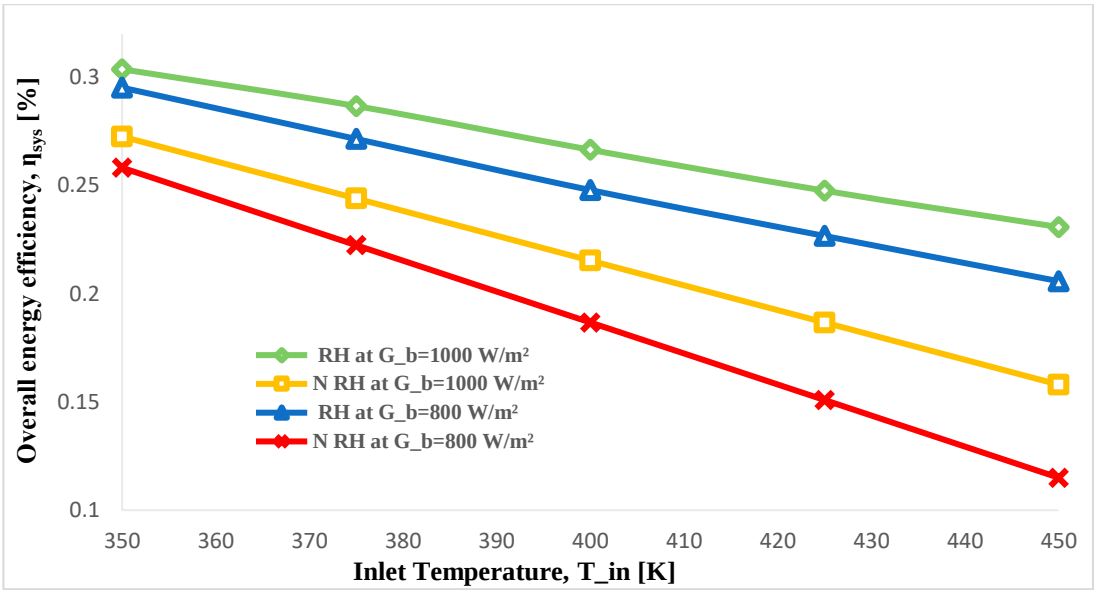

Figure 5.15: Effect of Inlet Temperature of Receiver on Overall Energy Efficiency of the Systems

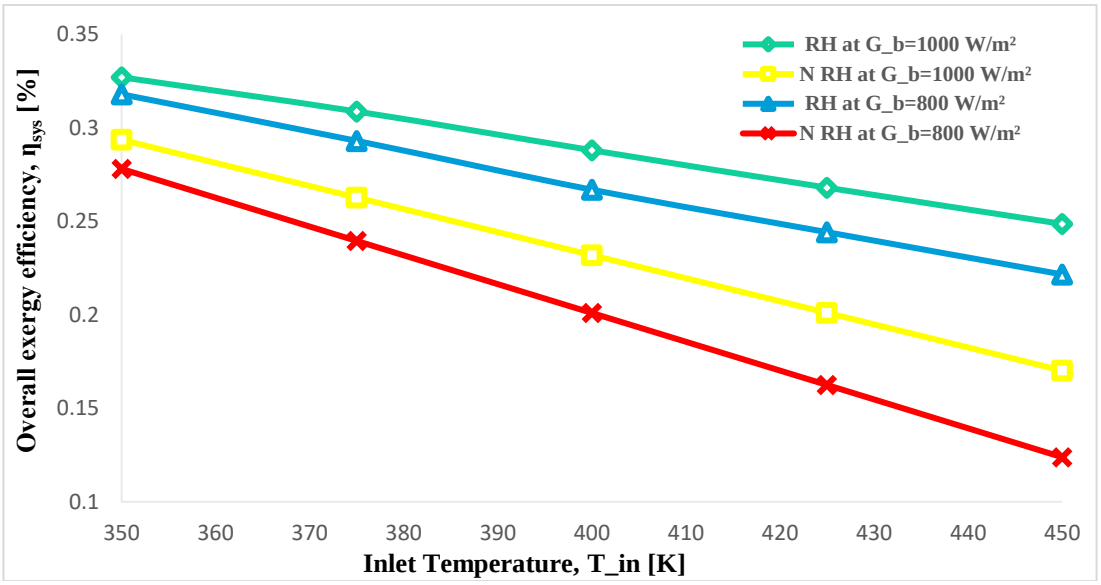

Figure 5.16: Effect of Inlet Temperature of Receiver on Overall Exergy Efficiency of the System

5.5 Effect of Turbine Inlet Temperature

Figure 5.17 represents that by enhancing the turbine inlet temperature (TIT), both systems exhibit positive behavior. For reheat system integrated energy and exergy efficiency increases linearly from 30.37% to 47.31% and 32.70% to 50.95%,

accordingly. The recompression without reheat system has showed the similar nature with low values than the reheat system.

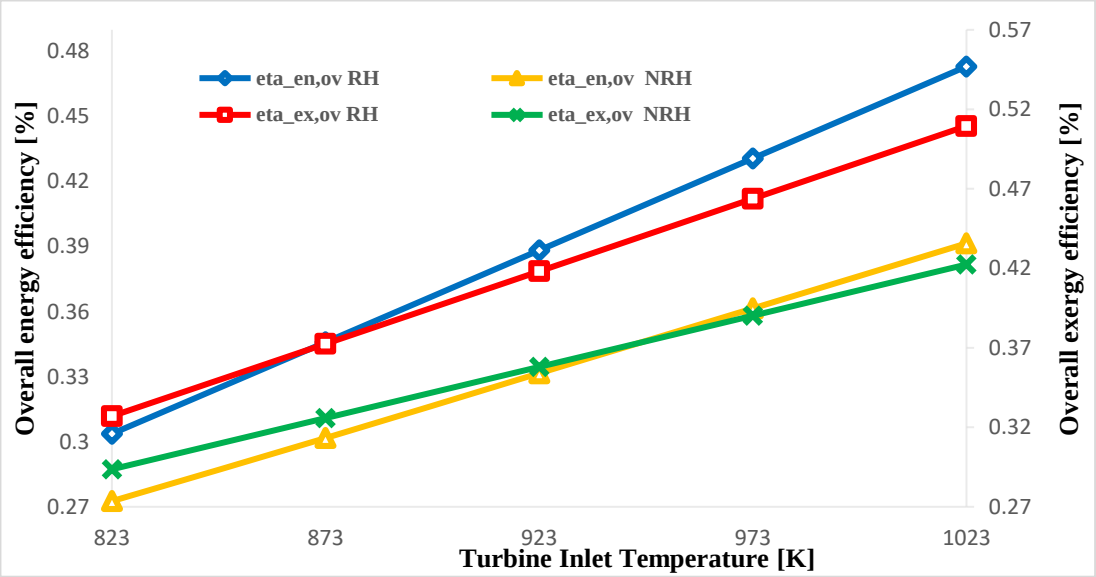

Figure 5.17: Turbine Inlet Temperature Effect on Overall Efficiencies of the Integrated Systems

5.6 Effect of Minimum Cycle Temperature

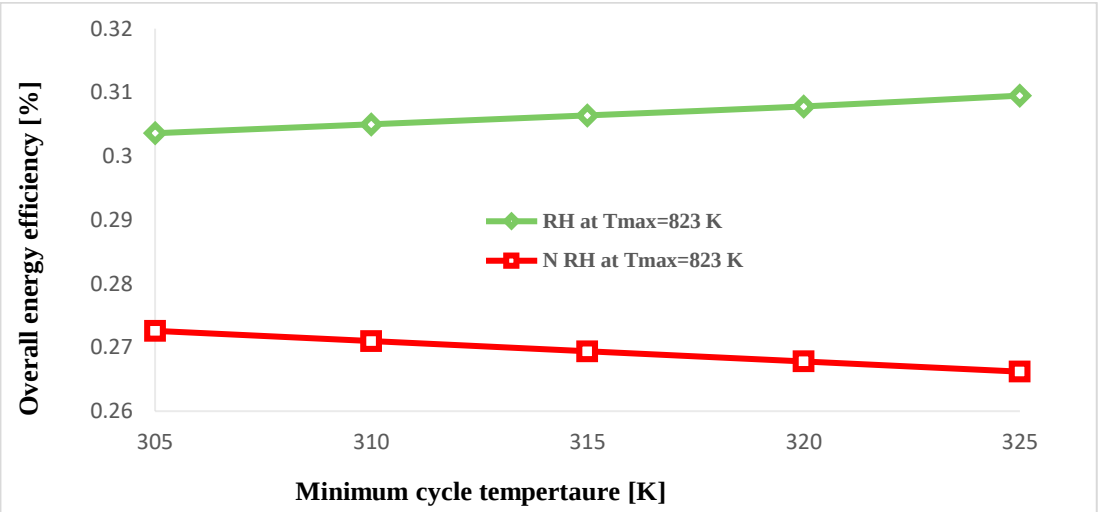

Figure 5.18: Effect of Minimum Cycle Temperature on Overall Energy Efficiency

The overall energy efficiency of the integrated solarized S-CO_2 recompression without reheat Brayton system decrease when minimum cycle temperature is increased but for recompressed reheat system it increases slightly as given in Figure 5.18. As the inlet temperature of without reheat system rises, work done by main compressor is also enhanced but turbine work and recompressing recompressor work almost remain constant as they are away from the critical point. So the power produced by the turbine is decreased that leads to reduction in net work output. Hence the overall energy efficiency for without reheat system reduces from almost 27.26% to 26.62%.

However, in the reheat integrated system the second turbine plays a substantial role to maintain the efficiency of system (as it increases the power) by compensating the increase in main compressor work. Thus the overall energy efficiency of reheat system slightly improves from 30.36 % to 30.95% by increasing the turbine inlet temperature and given in Figure 5.18.

5.7 Effect of Pressure Ratio

The effect of pressure ratio on the overall energy efficiencies of with reheat and without reheat solarized S-CO_2 Brayton systems are presented in Figure 5.19. As pressure ratio increases, efficiency of the both systems is increasing. But after the critical point (2.6), the efficiency of the recompression without reheat system is decreased slightly because of the increment in main compressor work that leads to decrease the cycle net work output. But in the case of reheat system, again the second turbine helps to maintain the system efficiency after the increase in main compressor work. That's why reheat system has an overall energy efficiency in an improved mode.

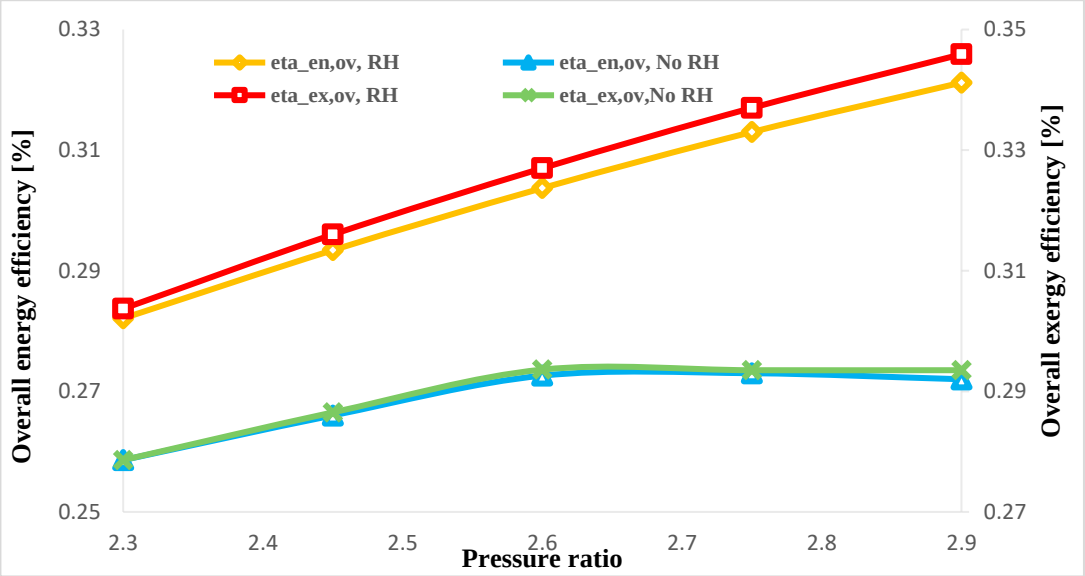

Figure 5.19: Effect on Overall Efficiencies due to the Variation in Pressure Ratio

5.8 Effect of Maximum Cycle Pressure

Figure 5.20 shows the effect of compressor outlet pressure on the overall energetic and exergetic efficiencies of both systems. Efficiency values of the both integrated systems increase by enhancing the maximum cycle pressure as all compressors and turbines work also rise but increase in turbine work is significantly more as compared to the main compressor work. Therefore, net work out put increases which gives more efficiency. But for the value of higher pressures, the improvement in overall energy efficiency values is not significant due to the diversion of the system from critical point. Finally, systems efficiencies are increasing in the beginning but very less increment is found due to the recompressed fraction of mass attains its highest value.

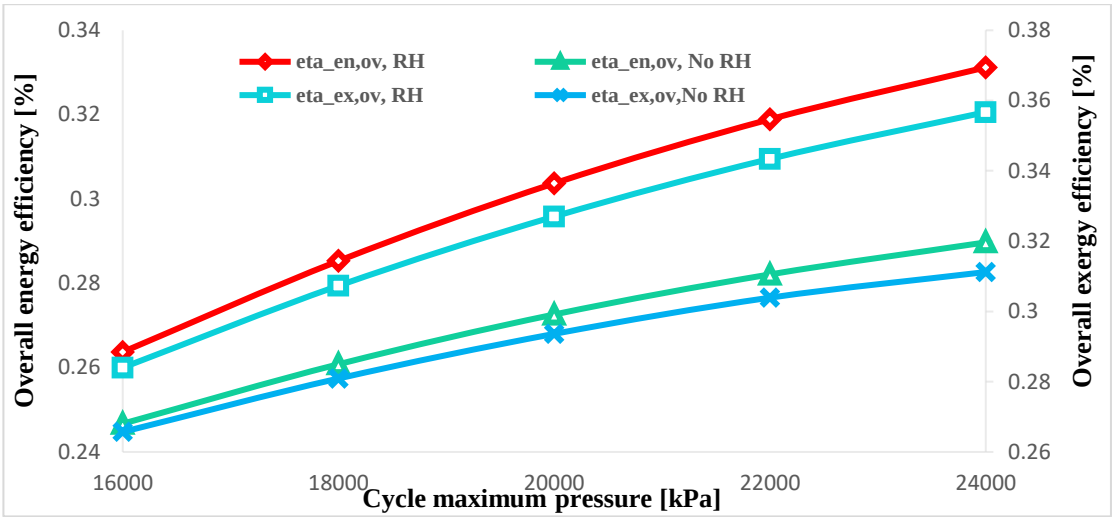

Figure 5.20: Compressor Outlet Pressure Effect on Overall Efficiencies of Integrated Systems

5.9 Exergy Destruction Rate

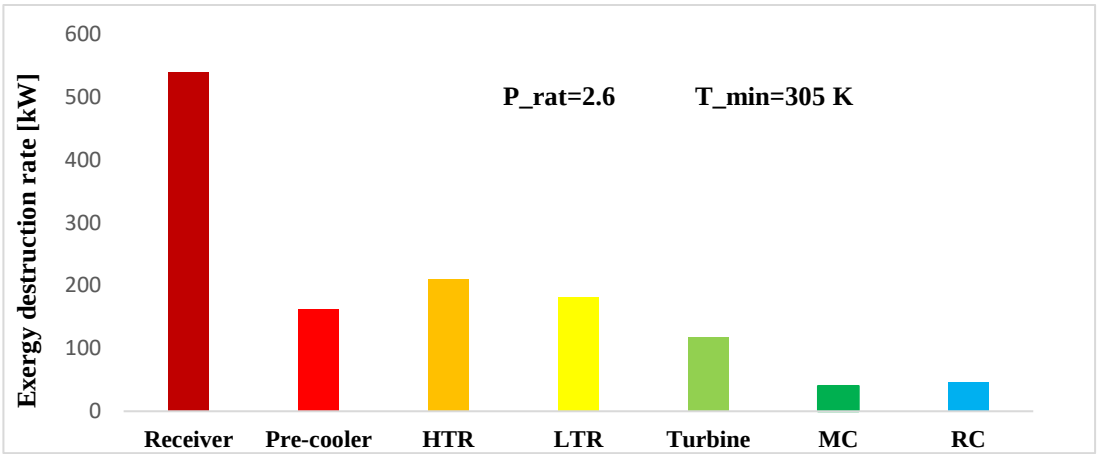

Figure 5.21 (a): Exergy Destruction Rate of Integrated System at T_min=305 K

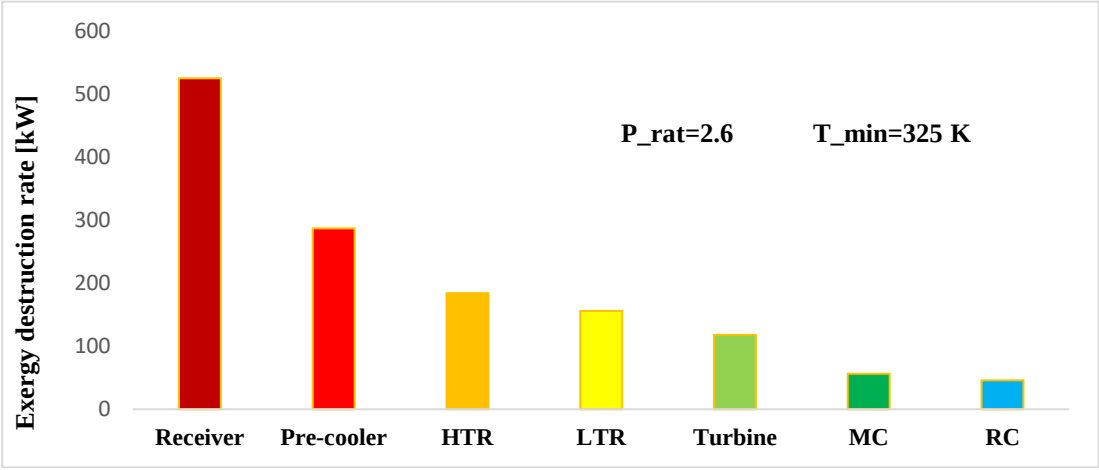

Figure 5.21 (b): Exergy Destruction Rate of Integrated System at T_min=325 K

Figure 5.21 (a) indicates that the rate of exergy destruction is higher in solar receiver, approximately 42%, while the HTR and LTR also have the maximum exergy destruction rate almost 16.2% and 14%, respectively. When minimum cycle temperature increases to 325 K, exergy destruction rate of pre cool increases dramatically from 12.5% to 22.12% as given in Figure 5.21(b), whereas, re compressor and turbine remain at same level. The exergy destruction rate of collector is decreased slightly just one percent and recuperators also have less exergy destruction rate by increasing the minimum cycle temperature.

5.10 Validation of the Results

The thermal efficiency of reheat recompression and without reheat recompression S-CO_2 Brayton cycles have been assessed at different inlet temperatures of the turbine as depicted in Figure 5.22. Former cycle has higher first law efficiency (47.70%), whereas, the latter gets efficiency approximately (45.02 %) showing a good agreement with the results obtained by [17, 18, 38]. This is the indication that the recompression, regeneration and reheating, introducing to S-CO_2 Brayton cycle is able to gain thermal efficiencies more than the ultra-supercritical (USC) plant [37], supporting its integration with solar system applications.

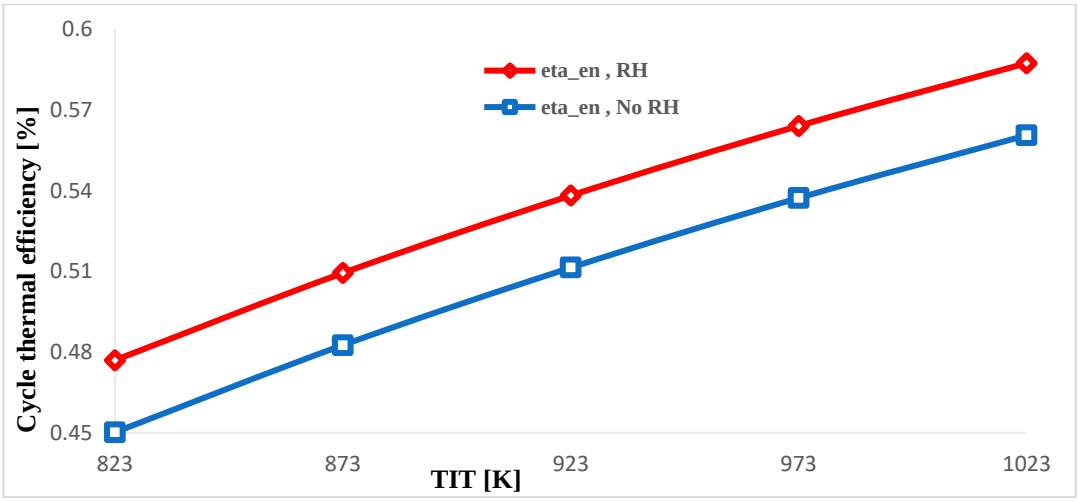

Figure 5.22: Turbine Inlet Temperature Effect on Thermal Efficiency of the Cycles

Table 5.1: Validation of current simulation with the published results [17, 18, and 38] for recompression without reheating S-CO_2 Brayton cycle

T_{min} (K)	T_{max} (K)	P_{max} (bar)	Pressure ratio	Present simulation	Reference
305	823	200	2.63	45.02	45.27 [17, 18]
305	1023	300	3.93	49.28	49.83 [38]

The PDSC model is analyzed for different values of inlet temperatures by conducting the parametric study and its influence on energy and exergy efficiency of the PD model.

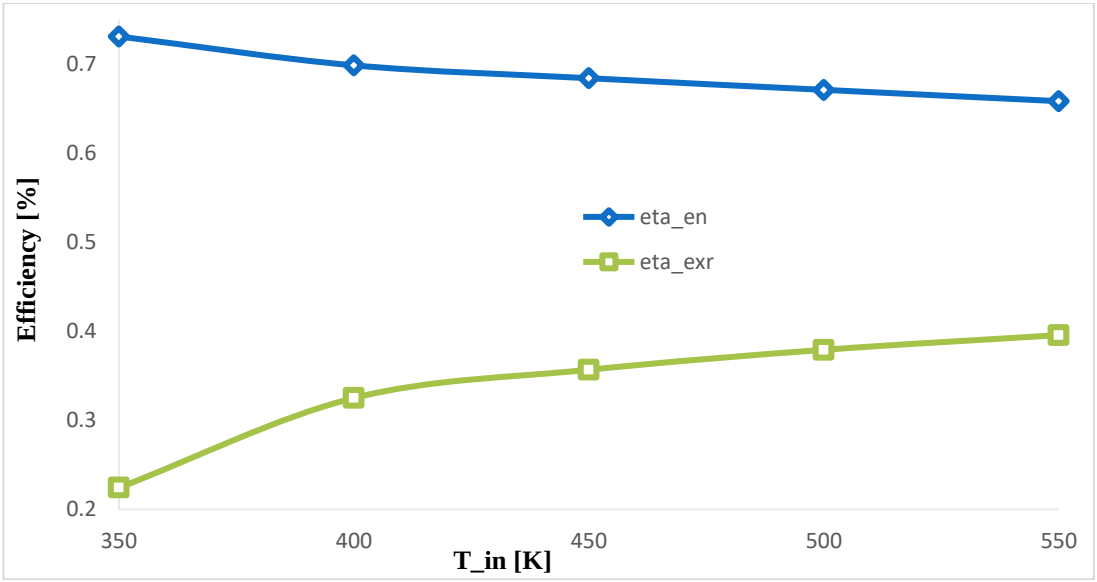

Figure 5.23: Effect of Receiver Inlet Temperature on Efficiency of PD Solar Collector

Moreover, results obtained from the study are compared and validated with the already publish results of [34], is given in table 5.2. The energy efficiency shows a decreasing trend by increasing the inlet temperature of the receiver because energy efficiency of receiver is ratio between rate of heat produced to energy available from solar and heat generation rate decreases when inlet temperature of receiver is increasing whereas, rate of solar energy remains constant. Finally, energy efficiency of collector is reduced. From collector exergy efficiency point of view, inlet temperature has direct relation which increases its exergy efficiency, and is given in Figure 5.23.

Table 5.2: Present Work Validation with the Ref. [34] at T_in = 350 K.

Source	η_{en}[%]	η_{ex}[%]	C_p (J / kg.K)
LIoyd C. Ngo [34]	73.11	16.52	4191
Present study	72.49	16.2	4181

Chapter 6

CONCLUSION AND FUTURE WORK

6.1 Conclusion

The present research describes the impact of the various operating parameters on the two different high efficiency thermodynamic cycles integrated with PDSC system. The parabolic dish system is analyzed and tested for its optical performance. The simulations of solar system is conducted on the annual based average DNI. Solarized integrated recompression with and without reheat S-CO_2 Brayton systems are compared for their overall efficiencies and net power outputs. Input parameters for both the S-CO_2 systems are kept the same throughout the modeling. The findings illustrate that the overall efficiencies are not enhanced linearly for higher values of maximum cycle pressure and almost remain constant due to the deviation of the system form critical behavior.

The recompression with reheat system has achieved the higher thermal efficiency and generated more power output for maximum value of DNI. The thermal efficiency of this cycle is almost 47.7%, whereas, integrated energy and exergy efficiencies are 30.37% and 32.7%, respectively. In addition, the recompression without reheat system has thermal, overall energetic and exergetic efficiencies around 45.02%, 27.5% and 29.6%, accordingly. Improvement in the overall performance is found nearly 10.5 % when reheat system is used. By increasing the inlet temperature of the receiver between 350 K and 450 K, system integrated energy and exergy efficiencies are reduced from

30.37% to 23.08 % and 32.7% to 24.86%, respectively for reheat cycle. The performance of both systems is improved for higher values of turbine inlet temperatures. By increasing the inlet temperature of the compressor, exergy destruction rate of main compressor is enhanced, while its impact on recompressor and turbine exergy losses is almost negligible. Solar receiver has the maximum exergy losses (40%), followed by recuperators.

6.2 Future Work

The present study is conducted to obtain the objectives that have been already set and during the process different points and slots have identified for future research. The other researchers can evaluate and improve the performance of the desired system by considering certain points in their study.

The other types of S-CO_2 Brayton cycles (pre compression, main compression with intercooling and partial cooling) shall be integrated and analyzed for their overall performance with PDSC. Nano fluids can also be used in solar collector and performance comparison can be made between direct and indirect heated integrated systems. The exergeoeconomic, envireconomic, exergoenvironmental and sustainability/ sensitivity analysis of the PDSC integrated with Brayton cycles can be the most important future workout. The exergoenvironmental impact analysis and rate of hydrogen production investigation can also be the major work in further development stages.

REFERENCES

[1] Schwarzbözl, P., Buck, R., Sugarmen, C., Ring, A., Crespo, M. J. M., Altwegg, P., & Enrile, J. (2006). Solar gas turbine systems: design, cost and perspectives. Solar Energy, 80(10), 1231-1240.

[2] Generation, R. P. (2013). Costs in 2012: An Overview/aut. IRENA. Emiratos Árabes Unidos: IRENA.

[3] Dostal, V., Driscoll, M. J., & Hejzlar, P. (2004). A supercritical carbon dioxide cycle for next generation nuclear reactors (Doctoral dissertation, Massachusetts Institute of Technology, Department of Nuclear Engineering).

[4] Feher, E. G. (1968). The supercritical thermodynamic power cycle. conversion, 8(2), 85-90.

[5] Cengel, Y. A., & Boles, M. A. (2002). Thermodynamics: an engineering approach. Sea, 1000, 8862.

[6] Kalogirou, S. A. (2013). Solar energy engineering: processes and systems. Academic Press.

[7] Vikram, T. S., & Reddy, K. S. (2014). Estimation of heat losses from modified cavity mono-tube boiler receiver of solar parabolic dish for steam generation. Energy Procedia, 57, 371-380.

[8] Palavras, I., & Bakos, G. C. (2006). Development of a low-cost dish solar concentrator and its application in zeolite desorption. Renewable Energy, 31(15), 2422-2431.

[9] Kaneff, S. (1998). Final Report on the Single, Large Dish Solar Thermal System for the New South Wales Department of Energy-1988-1998. Energy Research Center, ANUTECH Pty Ltd., Australia.

[10] Abid, M., Ratlamwala, T. A. H., & Atikol, U. (2016). Performance assessment of parabolic dish and parabolic trough solar thermal power plant using nanofluids and molten salts. International Journal of Energy Research, 40(4), 550-563.

[11] Ho, C. K., & Iverson, B. D. (2014). Review of high-temperature central receiver designs for concentrating solar power. Renewable and Sustainable Energy Reviews, 29, 835-846.

[12] Song, Y., Wang, J., Dai, Y., & Zhou, E. (2012). Thermodynamic analysis of a transcritical CO2 power cycle driven by solar energy with liquified natural gas as its heat sink. Applied energy, 92, 194-203.

[13] Wang, J., Zhao, P., Niu, X., & Dai, Y. (2012). Parametric analysis of a new combined cooling, heating and power system with transcritical CO2 driven by solar energy. Applied energy, 94, 58-64.

[14] Turchi, C. S., Ma, Z., & Dyreby, J. (2009, April). Supercritical CO2 for

application in concentrating solar power systems. In SCCO2 Power Cycle Symposium, RPI, Troy, NY (pp. 1-5).

[15] Dostal, V., Driscoll, M. J., & Hejzlar, P. (2004). A supercritical carbon dioxide cycle for next generation nuclear reactors (Doctoral dissertation, Massachusetts Institute of Technology, Department of Nuclear Engineering).

[16] Feher, E. G. (1968). The supercritical thermodynamic power cycle. Energy conversion, 8(2), 85-90.

[17] Sarkar, J. (2009). Second law analysis of supercritical CO2 recompression Brayton cycle. Energy, 34(9), 1172-1178.

[18] Sarkar, J., & Bhattacharyya, S. (2009). Optimization of recompression S-CO2 power cycle with reheating. Energy Conversion and Management, 50(8), 1939-1945.

[19] Akbari, A. D., & Mahmoudi, S. M. (2014). Thermoeconomic analysis & optimization of the combined supercritical CO2 (carbon dioxide) recompression Brayton/organic Rankine cycle. Energy, 78, 501-512.

[20] Niu, X. D., Yamaguchi, H., Zhang, X. R., Iwamoto, Y., & Hashitani, N. (2011). Experimental study of heat transfer characteristics of supercritical CO2 fluid in Collectors of solar Rankine cycle system. Applied Thermal Engineering, 31(6-7), 1279-1285.

[21] Zhang, X. R., & Yamaguchi, H. (2008). An experimental study on evacuated tube solar collector using supercritical CO2. Applied Thermal Engineering, 28(10), 1225-1233.

[22] Wright, S. A., Conboy, T. M., Parma, E. J., Lewis, T. G., & Suo-Anttila, A. J. (2011). Summary of the Sandia Supercritical CO2 Development Program (No. SAND2011-3375C). Sandia National Laboratories (SNL-NM), Albuquerque, NM (United States).

[23] Iverson, B. D., Conboy, T. M., Pasch, J. J., & Kruizenga, A. M. (2013). Supercritical CO2 Brayton cycles for solar-thermal energy. Applied Energy, 111, 57-970.

[24] Singh, R., Miller, S. A., Rowlands, A. S., & Jacobs, P. A. (2013). Dynamic Characteristics of a direct-heated supercritical carbon-dioxide Brayton cycle in Solar thermal power plant. Energy, 50, 194-204.

[25] Chacartegui, R., De Escalona, J. M., Sánchez, D., Monje, B., & Sánchez, T. (2011). Alternative cycles based on carbon dioxide for central receiver solar power plants. Applied Thermal Engineering, 31(5), 872-879.

[26] Al-Sulaiman, F. A., & Atif, M. (2015). Performance comparison of different supercritical carbon dioxide Brayton cycles integrated with a solar power tower. Energy, 82, 61-71.

[27] Turchi, C. S., Ma, Z., Neises, T. W., & Wagner, M. J. (2013). Thermodynamic

study of advanced supercritical carbon dioxide power cycles for concentrating solar power systems. Journal of Solar Energy Engineering, 135(4), 041007.

[28] Klein, S.A. (2009). Engineering Equation Solver, F-Chart Software. Madison, Wisconsin, v8.411.

[29] Besarati, S. M., & Goswami, D. Y. (2014). Analysis of advanced supercritical carbon dioxide power cycles with a bottoming cycle for concentrating solar power applications. Journal of Solar Energy Engineering, 136(1), 010904.

[30] Dincer, I., & Ratlamwala, T. A. H. (2013). Importance of exergy for analysis, improvement, design, and assessment. Wiley Interdisciplinary Reviews: Energy and Environment, 2(3), 335-349.

[31] Padilla, R. V., Too, Y. C. S., Benito, R., & Stein, W. (2015). Exergetic analysis of supercritical CO2 Brayton cycles integrated with solar central receivers. Applied energy, 148, 348-365.

[32] Adnan S, Khan AH, Haider S, Mahmood R. (2012). Solar energy potential in Pakistan. Journal of Renewable and Sustainable Energy, 4, 032701.

[33] Ebrahim, Zofeen T. (2015). World's largest solar park to light up Pakistan's future.

[34] Ngo, L. C. (2013). Exergetic Analysis and Optimization of a Parabolic Dish Collector for Low Power Application, Centre for Renewable and Sustainable

Energy Studies. University of Pretoria.

[35] Wu, S. Y., Xiao, L., Cao, Y., & Li, Y. R. (2010). A parabolic dish/AMTEC solar thermal power system and its performance evaluation. Applied Energy, 87(2), 452-462.

[36] Petela, R. (2010). Discussion of Radiation Exergy Formulae Proposed by Researchers. Engineering Thermodynamics of Thermal Radiation. McGraw-Hill, 247-263.

[37] Viswanathan, R., Coleman, K., & Rao, U. (2006). Materials for ultra-supercritical coal-fired power plant boilers. International Journal of Pressure Vessels and Piping, 83(11-12), 778-783.

[38] Yari, M., & Sirousazar, M. (2010). A novel recompression S-CO2 Brayton cycle with pre-cooler exergy utilization. Proceedings of the Institution of Mechanical Engineers, Part A: Journal of Power and Energy, 224(7), 931-946.

APPENDIX

EES CODES

```
T_0 =300

P_0 = 100

P[0]=P_0

T[0]=T_0

T_s = 5700

eta_0 = 0.85

F = 0.90{collector efficiency factor}

T_in =350

P_r_i=200

G_b = 1000

R = 1.8248

d = 0.20

D_a = 3^0.5*d

U_l = 150

m_dot_r= 0.004

P_d = 0.001

cp=Cp(Water,T=T_in,P=P_r_i)*1000

T_avg = (T_in + T_out)/2

A_a = Pi*R^2     {apurture area}

A_r = (Pi/4)*d^2

C = A_a/A_r

Col_r  = 1

"Q_dot_solar=(F_R*A_a*S*Col_r)"

Q_dot_solar =G_b*A_a

Q_l = Q_dot_solar - Q_dot_g

Q_l  = U_l*A_r*(T_r - T_0)

Q_dot_g = m_dot_r*Cp*(T_out - T_in)

Q_dot_g = F_R*A_a*(S - A_r/A_a*U_l*(T_in - T_0))
```

```
S = eta_0*G_b
F_R = (m_dot_r*Cp)/(A_r*U_l)*(1-exp(-(((A_r*U_l*F)/(m_dot_r*Cp)))))
Ex_dot_in = m_dot_r*Cp*(T_in - T_0 - T_0*Ln(T_in/T_0))
eta_pe = 1 - (4*T_0)/(3*T_s) + (1/3)*(T_0/T_s)^4
Ex_dot_solar  = G_b*A_a* eta_pe
Ex_dot_abs  = S*A_a* eta_pe
Ex_dot_out = m_dot_r*Cp*(T_out - T_0 - T_0*Ln(T_out/T_0))
Ex_dot_col  = Ex_dot_out  - Ex_dot_in
Q_dot_produced=Q_dot_g
"eta_en_PDSC=F_R*(eta_0-U_l*((T_out-T_0)/(G_b*C)))"
eta_ex_PDSC = Ex_dot_col/Ex_dot_solar
eta_en_PDSC=Q_dot_produced/Q_dot_solar
P[1]=76*100          "optimization of recompression s-co2 cycle with reheating bhatta"
P[2]=200*100
T[1]=305
T[5]=824
P_ratio=P[2]/P[1]
k=1.285
T[2]=388
T[3]=534
T[4]=658
T[6]=693
T[7]=T[5]
T[8]=T[6]
T[9]=556
T[10]=411
P[6]=9237.85
P[6]=P[7]
P[1]=P[10]
P[10]=P[9]
P[9]=P[8]
```

```
P[2]=P[3]
P[3]=P[4]
P[4]=P[5]
h[0]=Enthalpy(CarbonDioxide,T=T[0],P=P[0])
h[1]=Enthalpy(CarbonDioxide,T=T[1],P=P[1])
h[2]=Enthalpy(CarbonDioxide,T=T[2],P=P[2])
h[3]=Enthalpy(CarbonDioxide,T=T[3],P=P[3])
h[4]=Enthalpy(CarbonDioxide,T=T[4],P=P[4])
h[5]=Enthalpy(CarbonDioxide,T=T[5],P=P[5])
h[6]=Enthalpy(CarbonDioxide,T=T[6],P=P[6])
h[7]=Enthalpy(CarbonDioxide,T=T[7],P=P[7])
h[8]=Enthalpy(CarbonDioxide,T=T[8],P=P[8])
h[9]=Enthalpy(CarbonDioxide,T=T[9],P=P[9])
h[10]=Enthalpy(CarbonDioxide,T=T[10],P=P[10])
s[0]=Entropy(CarbonDioxide,T=T[0],P=P[0])
s[5]=Entropy(CarbonDioxide,T=T[5],P=P[5])
s[1]=Entropy(CarbonDioxide,T=T[1],P=P[1])
s[2]=Entropy(CarbonDioxide,T=T[2],P=P[2])
s[3]=Entropy(CarbonDioxide,T=T[3],P=P[3])
s[4]=Entropy(CarbonDioxide,T=T[4],P=P[4])
s[6]=Entropy(CarbonDioxide,T=T[6],P=P[6])
s[7]=Entropy(CarbonDioxide,T=T[7],P=P[7])
s[8]=Entropy(CarbonDioxide,T=T[8],P=P[8])
s[9]=Entropy(CarbonDioxide,T=T[9],P=P[9])
s[10]=Entropy(CarbonDioxide,T=T[10],P=P[10])
"HTR"
"epsilon_HTR=(T[8]-T[9])/(T[8]-T[3])"

epsilon_HTR=0.963
"epsilon_HTR=epsilon_LTR"
"LTR"
```

(1-x)*(h[3]-h[2])=(h[9]-h[10])

"epsilon_LTR=(T[9]-T[10])/(T[9]-T[2])"

epsilon_LTR=0.921

"Reactor"

"x=0.40"

m_dot=Q_dot_add/((h[5]-h[4])+(h[7]-h[6]))

"m_dot=Q_dot_add/((h[5]-h[4]))"

"Q_dot_add=4704"

m_dot=19.6

" Fahad Al- Sulaiman & Maimoon atif"

"compressors"

W_dot_mc=m_dot*(1-x)*(h[2]-h[1])

W_dot_rc=m_dot*(x)*(h[3]-h[10])

eta_mc=0.89

eta_mc=eta_rc

"Turbines"

W_dot_hpt=m_dot*(h[5]-h[6])

W_dot_lpt=m_dot*(h[7]-h[8])

W_dot_tur=W_dot_hpt+W_dot_lpt

eta_lpt=0.90

eta_hpt=eta_lpt

"pre-cooler"

Q_pc=m_dot*(1-x)*(h[10]-h[1])

W_dot_net=(W_dot_hpt+W_dot_lpt)-(W_dot_mc+W_dot_rc)

"W_dot_net=(W_dot_hpt)-(W_dot_mc+W_dot_rc)"

"eta_th=W_dot_net/Q_dot_add"

eta_th=47.7

"Exergy analysis"

Ex_in=Q_dot_add*(1-T[0]/T_ra)

T_ra=1073

```
Ex_dot[1]=m_dot*(1-x)*((h[1]-h[0])-T[0]*(s[1]-s[0]))
Ex_dot[2]=m_dot*(1-x)*((h[2]-h[0])-T[0]*(s[2]-s[0]))
Ex_dot[3]=m_dot*((h[3]-h[0])-T[0]*(s[3]-s[0]))
Ex_dot[4]=m_dot*((h[4]-h[0])-T[0]*(s[4]-s[0]))
Ex_dot[5]=m_dot*((h[5]-h[0])-T[0]*(s[5]-s[0]))
Ex_dot[6]=m_dot*((h[6]-h[0])-T[0]*(s[6]-s[0]))
Ex_dot[7]=m_dot*((h[7]-h[0])-T[0]*(s[7]-s[0]))
Ex_dot[8]=m_dot*((h[8]-h[0])-T[0]*(s[8]-s[0]))
Ex_dot[9]=m_dot*((h[9]-h[0])-T[0]*(s[9]-s[0]))
Ex_dot[10]=m_dot*((h[10]-h[0])-T[0]*(s[10]-s[0]))
"Exergy destruction"
Ex_dot_dest_mc=W_dot_mc -((1-x)*(Ex_dot[2]-Ex_dot[1]))
Ex_dot_dest_rc=W_dot_rc-x*(Ex_dot[3]-Ex_dot[10])
Ex_dot_dest_hpt=(Ex_dot[5]-Ex_dot[6])-W_dot_hpt
Ex_dot_dest_lpt=(Ex_dot[7]-Ex_dot[8])-W_dot_lpt
Ex_dot_dest_pc=(1-x)*Ex_dot[10]-Ex_dot[1]
Ex_dot_dest_ltr=(Ex_dot[9]-Ex_dot[10])-(1-x)*(Ex_dot[3]-Ex_dot[2])
Ex_dot_dest_htr=(Ex_dot[8]-Ex_dot[9])-(Ex_dot[4]-Ex_dot[3])
Ex_dot_dest_react=Ex_dot[4]-Ex_dot[5]+Ex_dot[6]-Ex_dot[7]+Ex_in
"exergy efficiency"
eta_exrg=W_dot_net/Ex_in
eta_ex_ov=W_dot_net/Ex_dot_solar
eta_en_ov=W_dot_net/Q_dot_solar
```